Beam Research Program

April 1984

LLL TB 63

Energy and Technology Review Reprints
Lawrence Livermore National Laboratory

Cover Description

Technician checks water feed lines just beyond the final accelerator module of the Advanced Test Accelerator located at LLNL Site 300. The vertical, black pipes are transmission lines, which deliver 250 kV, 70 ns pulses to the individual accelerator modules, each of which adds an increment of kinetic energy to the beam. Having reached its final design energy of 50 MeV, the beam will be transported from the final accelerator module into experimental chambers that will test its propagation characteristics in a variety of gases.

Beam Research Program

April 1984

LLL TB 63

Energy and Technology Review Reprints
Lawrence Livermore National Laboratory

Foreword

Charged-particle beams represent an application of pulsed power technology that promises a potential military breakthrough. Their future use as weapons depends on the feasibility of propagating intense, self-focused beams through the atmosphere. The current DARPA Particle Beam Technology Program is aimed at answering these feasibility issues with the Experimental Test Accelerator (ETA) and Advanced Test Accelerator (ATA) facilities at the Lawrence Livermore National Laboratory.

The articles that follow review ongoing work in many facets of the Laboratory's Beam Research Program. The ETA, which provides the technology base for the ATA, is described in "Accelerating Intense Electron Beams." The ATA mode of operation, design, and military application potential is described in "Generating Intense Electron Beams for Military Applications." Possible use of such electron beams for efficiently generating intense beams of laser radiation is discussed in "The Free-Electron Laser Amplifier." Ongoing research to develop pulse power generators that are more reliable and maintainable than the spark-gap technology currently used on ATA is reviewed in "Magnetic Compressors: High-Power Pulse Sources."

Accelerating Intense Electron Beams

Following nearly 20 years of research and development in the field of intense particle beams, we have built a new experimental test accelerator incorporating several technological innovations. The program is sponsored and funded by the Defense Advanced Research Projects Agency (DARPA). The unusual feature of this accelerator is its remarkable combination of characteristics: moderate electron energy (5 MeV), high current (10 kA), short pulse length, 1-kHz repetition rate burst mode, and excellent beam quality. The linear-induction technology of the experimental accelerator may be readily extended for the production of higher energy beams; the current experimental accelerator will provide the technology base for the injector for an even more advanced (50-MeV) accelerator, also sponsored by DARPA.

During the past several years, the applied-physics research community has sought to exploit rapidly developing pulsed-power technology to satisfy major national needs. Like the magnetic and laser fusion programs, the beam-research program has extended this technology through its efforts in producing relativistic electrons by means of an electron accelerator.

An electron accelerator applies a local electric field to a cluster of traveling electrons, accelerating the electrons through the structure. In this way, the electrons continuously or successively acquire energy until their total energy is

For further information contact William A. Barletta (415) 422-6705.

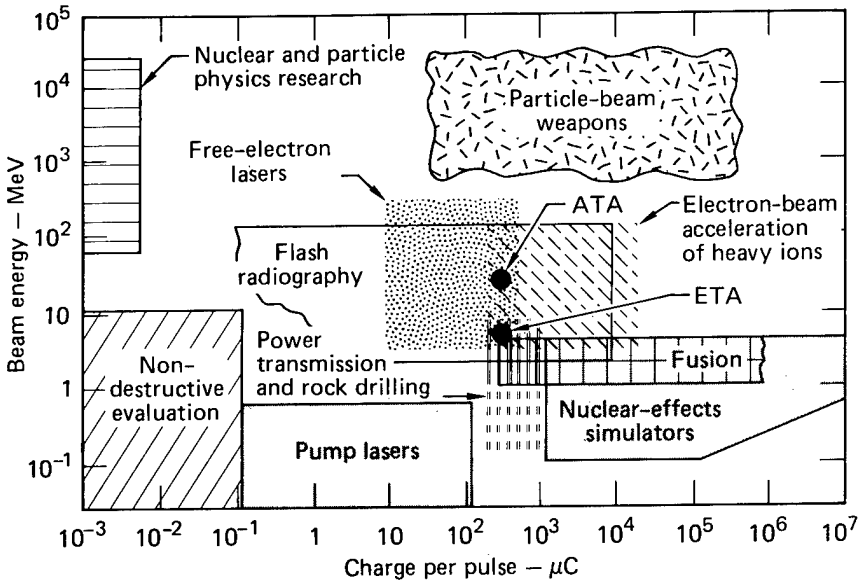

Fig. 1

Possible applications of electron-beam accelerators. Applications of pulsed electron beams may be characterized by the required beam energy and charge per pulse (the product of pulse length and current). The experimental test accelerator (ETA), stands at the crossroads for application to a number of scientific and technological needs.

many times their rest energy and their velocity is very close to the velocity of light.

Recent advances in pulsed power have made feasible a number of high-technology applications with intense electron beams. Under DARPA sponsorship and funding, we are conducting theoretical and experimental studies of intense beam physics relevant to military applications. Of a wide variety of possible uses of electron beams, electron-beam fusion and beam-weapon applications have received recent public attention and media coverage. A less widely heralded application, the free-electron laser, has recently attracted considerable interest in the scientific community.[1]

Figure 1 illustrates several applications for electron beams, defined by their beam parameters. The illustration does not distinguish regions of early research from regimes of final application, nor does it exhaust the possible applications.

Our most recent addition to electron-beam technology is a new facility, the 5-MeV experimental test accelerator (ETA), illustrated in Fig. 2. This facility combines several recent innovations with our nearly 20 years of experience in accelerating intense electron beams. As Fig. 1 shows, the ETA stands at a crossroads of applications that include flash radiography,[2] inertial fusion, and heating of plasmas for magnetic fusion. More speculative applications are electric power transmission and rock drilling. Once perfected, the ETA technology will be used in the injector design for a 50-MeV advanced test accelerator.

Interest in the production of intense, high-quality electron beams at LLNL originated in about 1959 with the proposal of the ASTRON concept.[3] The key feature of this concept—whose principal purpose was the containment and heating of a plasma to thermonuclear burn conditions—was a cylindrical layer of electrons trapped in a solenoidal magnetic field. This concept required a repetitively pulsed, high-current beam of relativistic electrons to drive the system.

Fig. 2

Model of an early design for the ETA. We have recently completed construction of this 5-MeV experimental electron-beam accelerator, which embodies significant advances in the state of the art. The accelerator employs linear magnetic induction and other features developed for our ASTRON program. The initial voltage pulse is formed by a coaxial Blumlein transmission line (vertical cylinders) that is triggered by a spark discharge from an energy storage and charging network.The electron-beam pulse is produced by an electron injector that consists of an anode-cathode and a series of magnetic accelerating units. This beam pulse, or electron cluster, is fed into a post-accelerator that increases the electron energy up to the final desired value through a series of additional magnetic induction units. The beam is then guided by a beam-transport unit into an experimental tank, or test region.

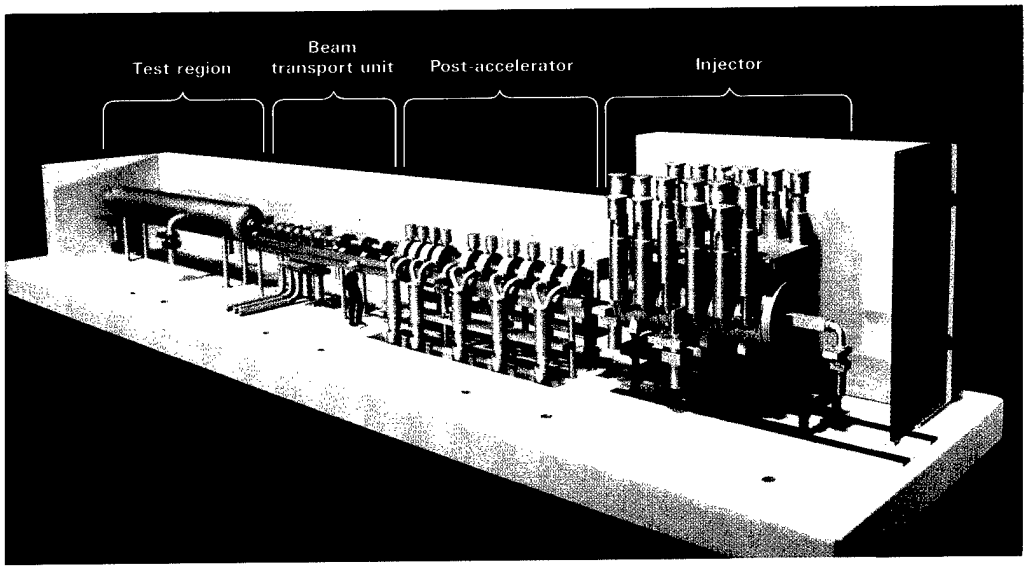

An examination of several types of existing accelerators led to the construction in 1963 of a linear accelerator (ASTRON I) based on the principle of magnetic induction. In such accelerators, accelerating voltages are produced by varying magnetic fields. A second, higher current linear-induction accelerator was built at LLNL in 1968. Following the termination of the ASTRON program in 1972, the ASTRON II accelerator continued to be a useful tool for study of beam-gas and beam-plasma interactions. The ASTRON II was dismantled in late 1976 and salvaged for the ETA.

ETA Operational Features

Construction of our ETA started in February 1977 on the site of the former ASTRON II. Our favorable experience with the ASTRON accelerator influenced our choice of the linear-induction concept to meet the operational requirements for ETA, which has a combination of desirable features:

- Moderate electron energy (5 MeV).
- High current (10 kA).
- Short pulse length (50 ns FWHM) at a 5-pulse/s rate.
- 1-kHz repetition-rate burst mode of 5 pulses in sequence spaced by 1 ms; when operating in this mode, the time-averaged repetition rate remains at 5 pulses/s.
- Excellent beam quality, a measure of the combination of small beam size and small angular divergence.

These operating features represent a significant improvement over existing high-current accelerator technology. Table 1 compares ETA parameters with those of ASTRON II and Lawrence Berkeley Laboratory's electron ring accelerator (ERA). The design of the ETA can be easily extended for the production of even higher energy beams.

Design Options and Choices

A qualitative description of the accelerator design options (for example, linear versus circular designs, radio-frequency or inductive acceleration) may explain the choice of a linear-induction accelerator for ETA.

Conceptually, the simplest electron accelerator is a pulsed diode, which consists of an electron source (cathode) and a positive electrode (anode) separated by a short vacuum region. When a pulse of very high voltage (up to several megavolts) is impressed across the gap, electrons are emitted from the cathode toward the anode. If the anode is a thin foil, the electron beam will pass through it into an experimental region.

Pulsed diodes have produced beams with energies as high as 12 MeV and currents exceeding 1 MA; the limiting energy value is determined by electrical breakdown of the insulating components. Unfortunately, the enormous currents of high-energy electrons damage the electrodes. Hence, such devices are used only for single, widely spaced shots. In practice, actual repetition rates range from a few shots per hour to a few shots per day.

To produce beams at rates in excess of 100 pulses/s at energies in excess of 12 to 15 MeV, we must consider more complex kinds of accelerators, such as the radio-frequency traveling-wave linear accelerator. Here, the accelerating electric field is a traveling electromagnetic wave rather than a single anode–cathode potential. The accelerator is basically a resonant waveguide structure designed to increase the velocity of the electron cluster as it moves down the structure from the source to the beam exit.

An important complication in any electron accelerator is that the self-generated electromagnetic fields of the electron cluster couple back into the

Table 1 Comparison of ETA with induction accelerator technology base.

	ASTRON II	ERA	ETA
Beam energy, MeV	6	4	4
Current, kA	0.8	1.2	10
Pulse length, ns	300	30	50
Burst rate, Hz	800	2	1000
Average rate, Hz	5	2	5

accelerator structure. This coupling effect can distort the accelerating fields and limit the output current. It can also cause small random perturbations in the beam's position or structure, which lead to damaging or current-limiting instabilities, as it does in the 20-GeV Stanford linear accelerator. Since the self-generated fields increase with increasing beam current, these considerations are especially serious for high-current accelerators, and most notably for circular (closed-loop) accelerators. Because the same charged particles are reaccelerated many times by the same electric field in a circular machine, the possibility of a high-current beam instability leading to catastrophic beam disruption is far greater than in linear accelerators. Furthermore, injection and extraction of the beam is more difficult than in linear accelerators.

The severity of the beam-structure interaction can be dramatically reduced by the choice of a linear array of nonresonant accelerating cavities, which operate on the principle of magnetic induction. In one form of the induction unit, the accelerating voltage appears across a gap in an axially symmetric metallic structure that encloses toroidal cores of ferromagnetic material (Fig. 3a).

Prior to the beam entering the cavity at time t_0, the cores are magnetized (set) to a maximum magnetic field, B_0 (Fig. 3b). At t_0, a voltage pulse, V_g, from the coaxial line (diagonal-line pattern in Fig. 3a) is impressed upon the accelerating gap. The ferrite acts as a large inductance, initially preventing a large current from flowing through the structure around the ferrite (dot pattern), thereby preventing the shorting of the coaxial line. In accord with the law of magnetic induction, this current increases at a steady rate given by the ratio V_g/ ferrite-inductance. In addition, the magnetic field decreases from its initial value, $+B_0$, at a constant rate until the field attains a minimum value, $-B_0$. At this time, the applied voltage pulse ends, and the wall current reaches its maximum value.

In addition to the time-varying fields that accelerate the electron cluster, static magnetic fields guide the beam as it moves down the accelerator from one cavity to the next.

For an induction accelerator, the area under the V_g-vs-t curve (volt-seconds) is a constant that depends only upon the value B_0 and the cross-sectional area, A, of the ferrite. If the beam pulse of length T is to be uniformly accelerated, the maximum voltage increase in each module is just $2B_0A/T$. The number of volt-seconds required to accelerate a pulse of given length determines directly the size of the accelerator cores.

In practice, the maximum accelerating voltage per module is often limited by the voltage-holding ability of the pulsed-power network that drives the accelerating cavity. Once the size and cost of an accelerator module are set, the size and cost of an induction accelerator are roughly proportional to the output voltage of the machine, beam pulse length being held constant.

An important factor in the operation of induction accelerators is the proper timing coordination of the voltage pulse to the accelerator module with the arrival of the electron cluster. Appropriate delays in the triggering circuits of the pulse-power network provide this timing.

The most unusual parameter of ETA, compared with previous linear-induction accelerators, is the high beam current, which has led to some special design features. Quantitative considerations of the type just discussed led us to choose an accelerator of the induction variety with toroidal ferrite cores. Furthermore, the prospect of accelerator instabilities led us to select high-voltage induction units similar to those in the Lawrence Berkeley Laboratory's accelerator rather than the lower voltage units used in the ASTRON design. This choice reduces the number of accelerator structures that can interact with the electron beam. The high current also requires a relatively high-voltage electron injector (2.5 MeV) to avoid serious beam-transport problems caused by the beam's self-generated fields. These fields have a net force that is the difference between the electrostatic self-repulsion of the electron cluster and the magnetic pinch forces that tend to

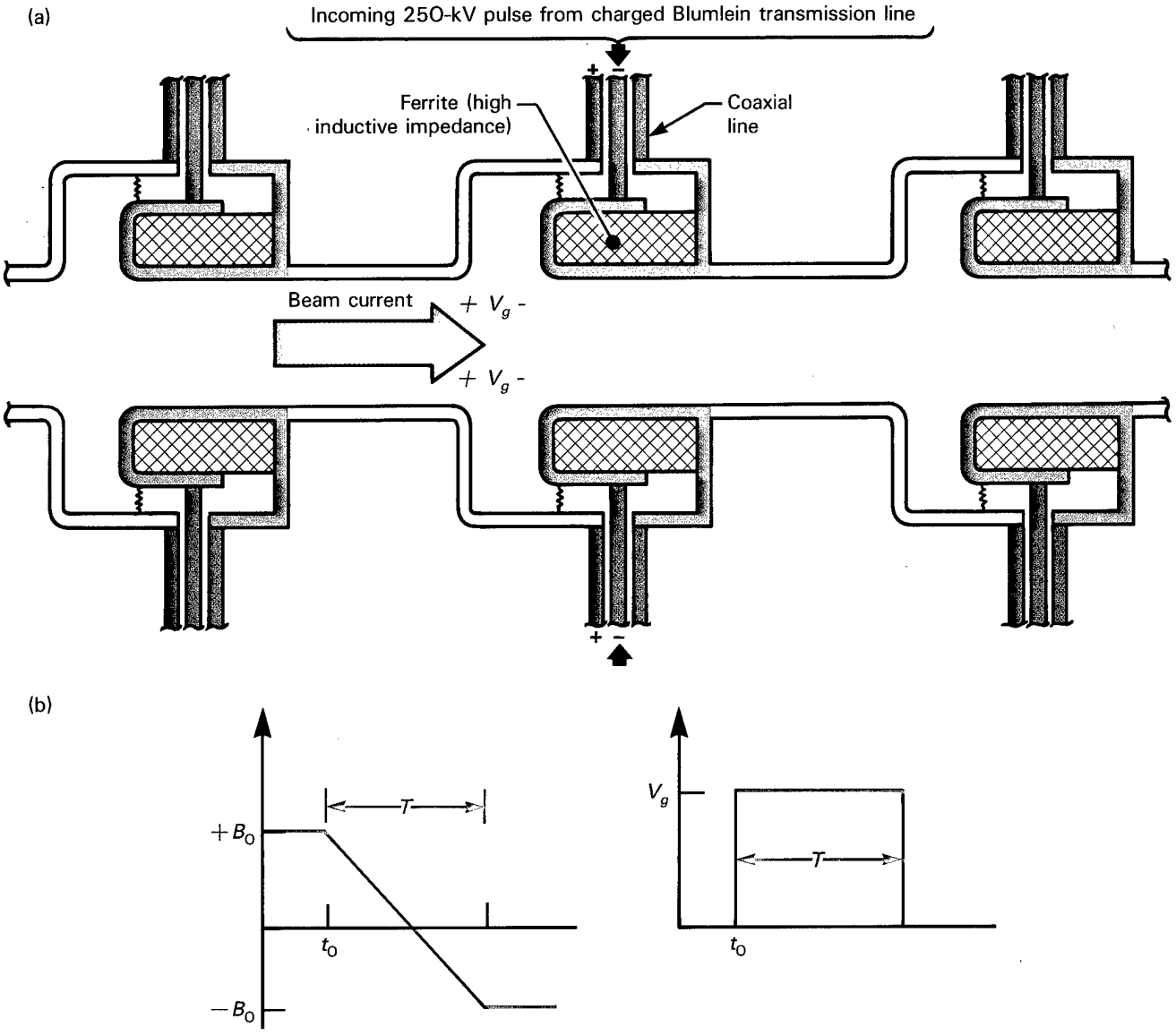

hold the beam together. For relativistic beams, these forces nearly cancel, with the repulsive net force proportional to the inverse square of the beam energy.

The linear electron accelerator consists of four major units: a pulse-forming network, an electron injector, a post-accelerator, and an experimental tank. It is the post-accelerator that contains the non-resonant cavities and is the heart of the linear electron accelerator. A relatively low-energy beam of desired pulse length is injected into the post-accelerator by the electron injector, which may or may not operate on the same principle as the post-accelerator. Once the beam is at its final energy at the terminal end of the post-accelerator, it is magnetically guided in a beam-transport unit to an experimental area.

Pulsed Power Network

Pulsed electrical power for the accelerator is provided by a pulse-forming network, which performs the process of energy compression: a discrete amount of energy is stored in a series of components over a period of time and is released suddenly. One such component may be an electrical transmission line that is charged to a desired voltage in much the same manner as a capacitor. A cylindrical three-conductor transmission line (Blumlein) is frequently used in pulsed electron accelerators.

Fig. 3

(a) Schematic of three accelerator modules of a linear-induction accelerator. Pulsed power is fed to the cavities by coaxial transmission lines (diagonal-line pattern). The accelerating voltage, V_g, appears across the gap for a time because the ferrite keeps the line from shorting by changing its magnetic field from a maximum B_0 to a minimum $-B_0$. Beam direction is to the right. (b) The time, T, during which the magnetic field changes from its maximum to minimum value is the longest length beam pulse that the module can accelerate. The magnitude of V_g is proportional to the slope of the B-vs-t curve.

Fig. 4

Pulsed electrical power for the accelerator units is provided by a pulse-forming network that converts ac power from a transformer substation into short, very high-voltage pulses. The key process is the charging of a Blumlein transmission line (similar to charging a capacitor) in a relatively long period and the subsequent fast discharge of the Blumlein in 1/200 of the time.

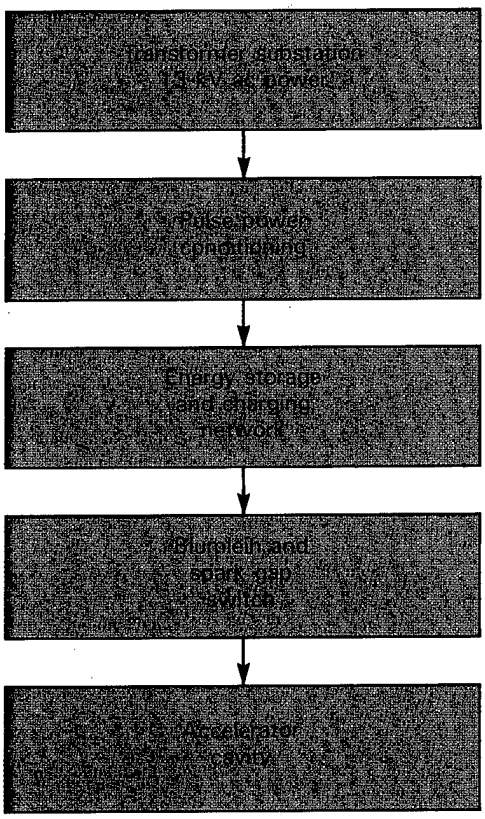

The power-flow and conditioning diagram in Fig. 4 demonstrates the actual conversion of energy from primary ac power to the beam. The ac power drives an energy-storage and charging network. The latter delivers a high-voltage pulse that is stepped up to 250 kV by a resonant transformer bolted to the Blumlein transmission line. Shortly after the current that has charged the Blumlein has dropped to zero, the spark gap switch is fired by a 150-kV trigger circuit. The resultant high-voltage output of the Blumlein is now impressed across the accelerating gap. As long as this pulse persists, electrons passing by the gap will be accelerated. The energy that took 10 μs to store in the Blumlein is delivered to the accelerating cavity in 50 ns, 200 times faster.

If a gas is flowed at high velocity through the spark gap switch, the Blumlein can be recharged and fired again at a 1-kHz burst rate. The voltage-holding ability of this switch—developed for ETA—determines the maximum accelerating voltage per ETA module. Because of limitations in the energy-storage subsystem, the spark gap is fired for a burst of five consecutive pulses with the burst repeated after 1 second.

Electron Injector

Accelerating voltages in both the electron injector and the post-accelerator are provided by similar power-supply and pulse-forming networks feeding the ferrite induction cores. The ETA's 2.5-MeV electron injector is a good example of the pulsed-power technology used in the accelerator as a whole.

Figure 5 is a schematic cross section of the electron injector. The electron source developed for ETA is a 25-cm-diam oxide-coated cathode, heated by a tungsten wire filament, capable of 50 A/cm^2 emission density and 20-kA total current. Our choice of a hot cathode was based on experience with the ASTRON accelerator, which demonstrated a high pulse-to-pulse reproducibility. As in a "standard" vacuum tube, a high-voltage pulse is applied to a grid to extract the required current from the cathode. The beam's self-generated electric field in the vicinity of the cathode is controlled by the grid (which shorts the beam's field) and by the solenoidal focusing coils.

The injector is constructed in two parts, each with five 0.25-MV induction units in series. Two large ceramic accelerating columns are each divided by metallic rings into ten increments, connected by power resistors to ensure proper voltage distribution across the column to avoid electrical breakdown. The accelerating columns also serve as the barrier between the vacuum of the accelerator beam area and the oil dielectric that fills the induction units. The division of the injector into two parts has several advantages: It provides a vacuum pumping port in the center of the injector, partially shields the ceramic insulators from the electron beam, and makes assembly easier.

Upon exiting the injector, the 2.5-MeV electrons are magnetically transported through ten post-accelerator cavities, each of which imparts 0.25 MeV to the beam. When the beam attains its final

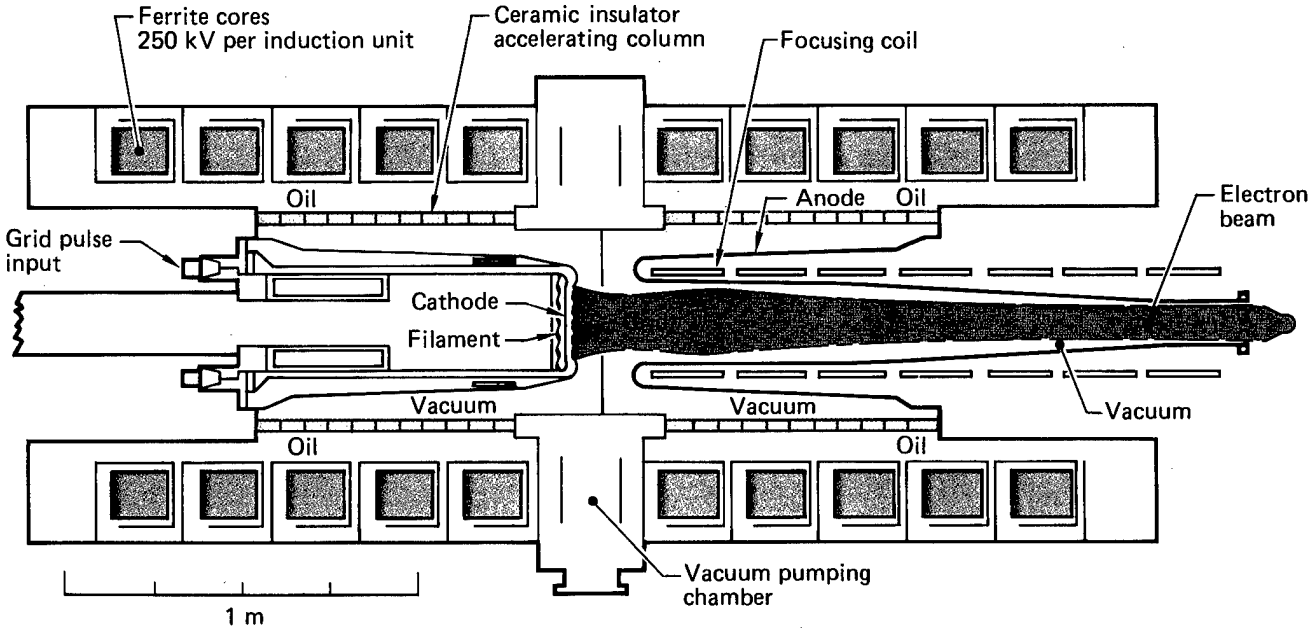

energy, it is magnetically guided into an experimental tank.

Future Directions

With the construction of the accelerator completed (see Fig. 6), we have begun our experimental program with measurements of beam current and voltage waveforms and their variation on a pulse-to-pulse basis. We will also measure the spatial distribution and angular divergence of the beam. Once we understand the nature of the beam and its pulse-to-pulse reproducibility, we will resume our studies of beam stability and dynamics as well as beam-gas and beam-plasma interactions.

For all such studies we require accurate measurements. The accelerator

Fig. 5

A schematic of the 2.5-MeV electron injector for the ETA. The 2.5 MV between the anode and cathode (provided by ten induction accelerator units of 0.25 MV each connected in series) extracts 10 000 A from a large heated cathode. Focusing coils reduce the radius of the beam for injection into the post-accelerator.

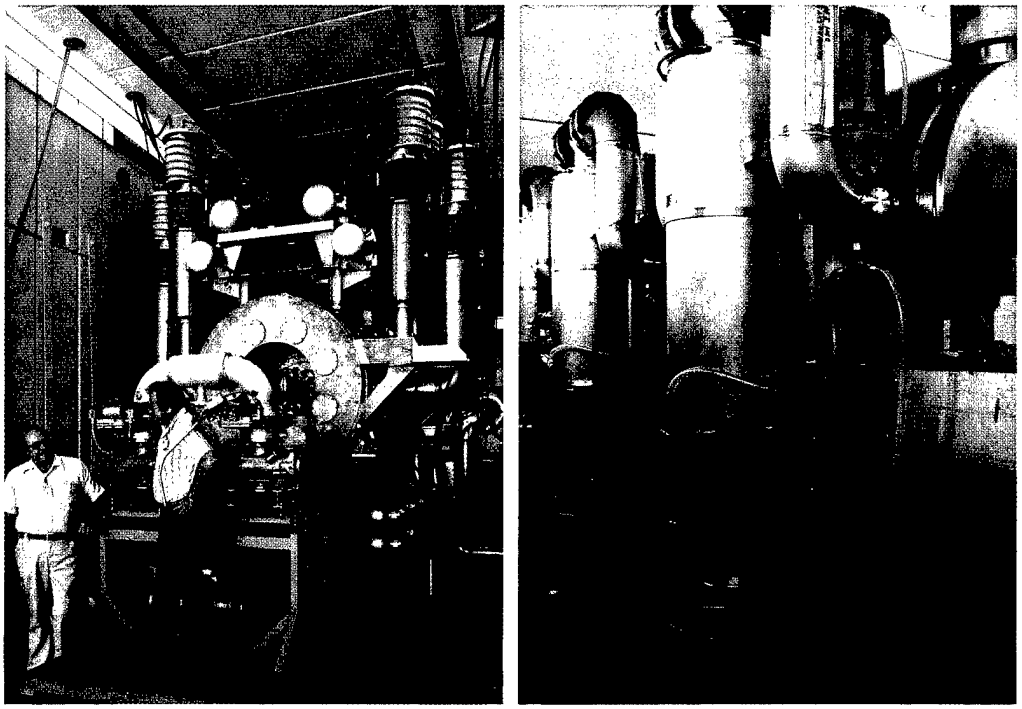

Fig. 6

Two views of the experimental test accelerator. (a) Electron injector and pulse-forming network. The large central cylinder houses the cathode structure and ferrite cores of the induction accelerators. Pulsed power is fed to the cores by the upright cylindrical Blumlein structures. On top of the Blumleins (in blue) are the high-pressure gas spark-gap switches and the transformers wound with cooling coils. (b) Post-accelerator. Because the electron beam is much smaller in diameter in the post-accelerator, these induction units are much smaller.

has been outfitted with a complete set of diagnostics, which includes a number of voltage and current probes designed specifically for ETA. In addition, the experimental tank diagnostics will include an x,y,z Faraday cup, laser interferometers, accoustic probes, and television systems.

The ETA will provide the technology for the electron injector for a higher-energy advanced test accelerator (ATA). By adding 180 more accelerating cavities to ETA, we will produce a 50-MeV, 10-kA electron beam. ATA is scheduled for completion in mid-1982 and will be located at Site 300. With its unique combination of high energy, current, and repetition rate, ATA promises to provide new applications for pulsed beams.

Key Words: accelerator; advanced test accelerator (ATA); ASTRON; beam research; Blumlein; electron accelerator; electron beams; electron injector; experimental test accelerator (ETA); linear accelerator; post-accelerator; pulsed electron beams.

Notes and References

1. In a free-electron laser, the electron beam passes through a region of magnetic field with varying intensity and direction while at the same time being illuminated by a laser. If one chooses the magnetic field, laser frequency, and beam energy properly, the electrons will emit radiation that amplifies the original laser pulse. The attractive feature of the free-electron laser is its potential to provide a tunable, high-power laser amplifier at visible and near-ultraviolet wavelengths. A direct application of such a laser is isotope separation.
2. For a brief status report of the Laboratory's high-explosive flash-radiography facility, see the January 1979 *Energy and Technology Review* (UCRL-52000-79-1), p. ii.
3. The ASTRON concept, proposed by the late N. C. Christofilos, is described in a survey of the Laboratory's magnetic fusion research for the first 25 years, presented in the May 1978 *Energy and Technology Review* (UCRL-52000-78-5), p. 1.

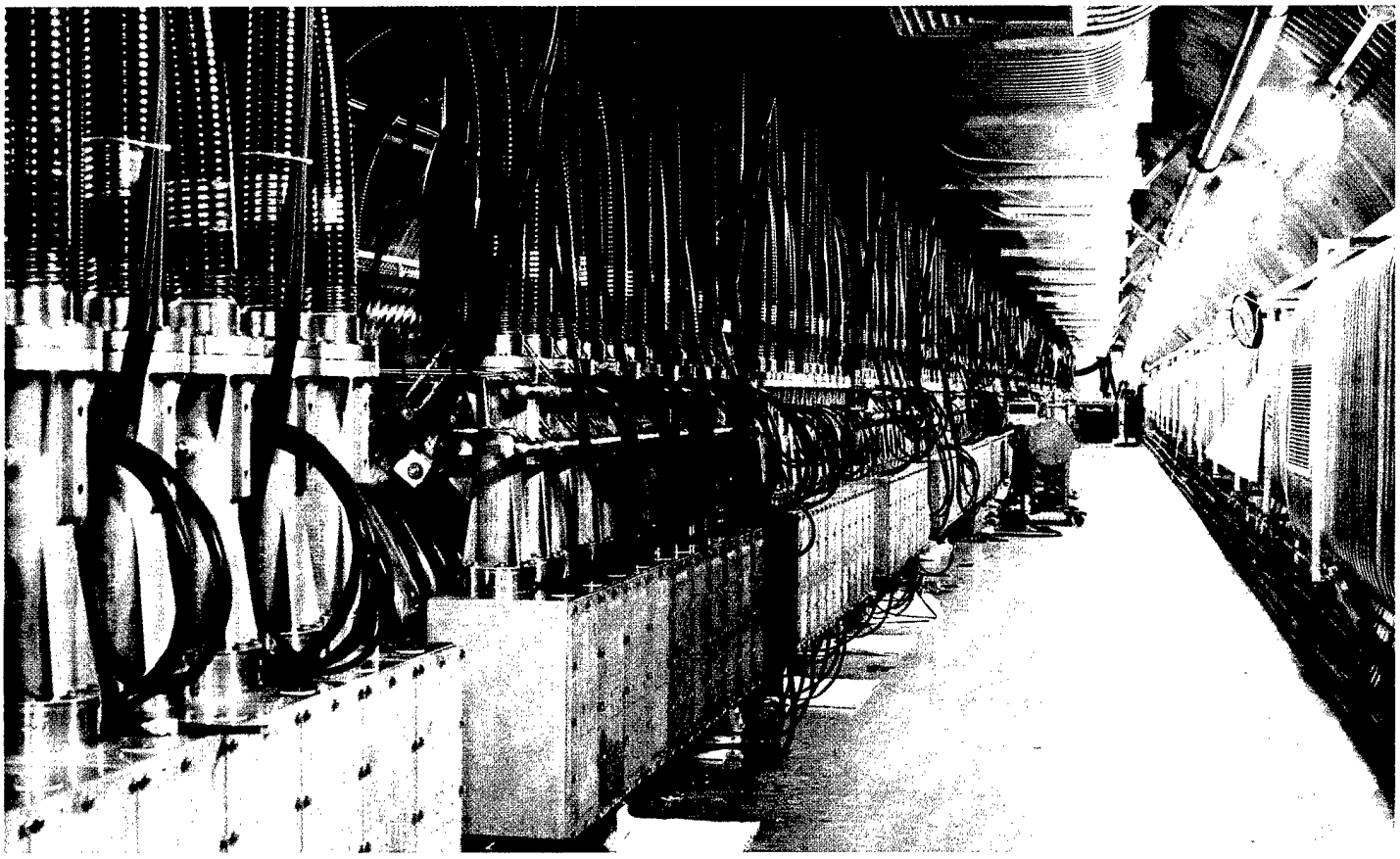

Generating Intense Electron Beams for Military Applications

The ATA Facility we are building at Site 300 will allow us to determine the feasibility of propagating intense, self-focused electron beams in the open air and to answer questions about their potential military applications.

Although charged-particle beams represent a potential breakthrough in military capability, their future use as weapons depends on the feasibility of propagating an intense, electromagnetically self-focused electron beam through the atmosphere. LLNL researchers hope to determine this by conducting a comprehensive program of electron-beam propagation experiments

For further information contact W. A. Barletta (415) 422-6705.

in a 50-MeV Advanced Test Accelerator Facility (the ATA)[1] that we are constructing at our high-explosives test location, Site 300. This facility, the successor to LLNL's Astron II and Experimental Test Accelerator (ETA), will cost about $50 million and should be completed by the fall of 1982.

The ATA, together with its associated program of beam-propagation physics, represents the largest single component of the Particle-Beam Technology Program conducted by the Defense Advanced Research Projects Agency (DARPA). This program was formerly sponsored by the U.S. Navy, and the Naval Surface Weapons Center is now the direct funding agency for the DARPA program. The aim of this program of research and exploratory development is to resolve those scientific issues necessary to show that particle-beam weapons are possible. The prime goal of the DARPA Particle-Beam Technology Program is to resolve what is and is not possible in beam propagation. Accordingly, our goal with the ATA is to develop an experimental capability that can answer critical questions about beam-propagation physics in a timely and cost-effective fashion.

Although we can study many aspects of beam stability and propagation in a shielded experimental gas-filled tank, it is essential to test particle beams in open air to determine how the beam will propagate in various natural environments. In addition, we must be able to fire the beam in a range of directions to test methods of pointing and tracking. Finally, an outdoor facility will allow us to detonate safely substantial quantities of chemical explosives in target-damage studies.

Potential hazards associated with the ATA experiments were considered in choosing our site. LLNL's Site 300 is located in a remote area 25 km southeast of LLNL that is well equipped for managing such experiments. The ATA is being built in a shallow valley to exploit natural shielding. Figure 1 shows the ATA facility under construction.

Applications of Intense Beams

Recent advances in pulsed-power technology, notably the development of repetition-rated electrical components (i.e., ones capable of delivering short pulses of high-voltage, high-current electrical power many times per second), have made feasible a number of high-technology uses for intense electron beams. Of the wide variety of possible applications, flash radiography and nuclear effects simulation have considerable military significance. In their application in the free-electron laser, such

Fig. 1

ATA facility under construction at Site 300. The large corrugated metal tube (a) enclosing the experimental tank—exposed when this photograph was taken in April 1981—is now (b) covered with earth and concrete. The facility is scheduled to begin operation in the fall of 1982.

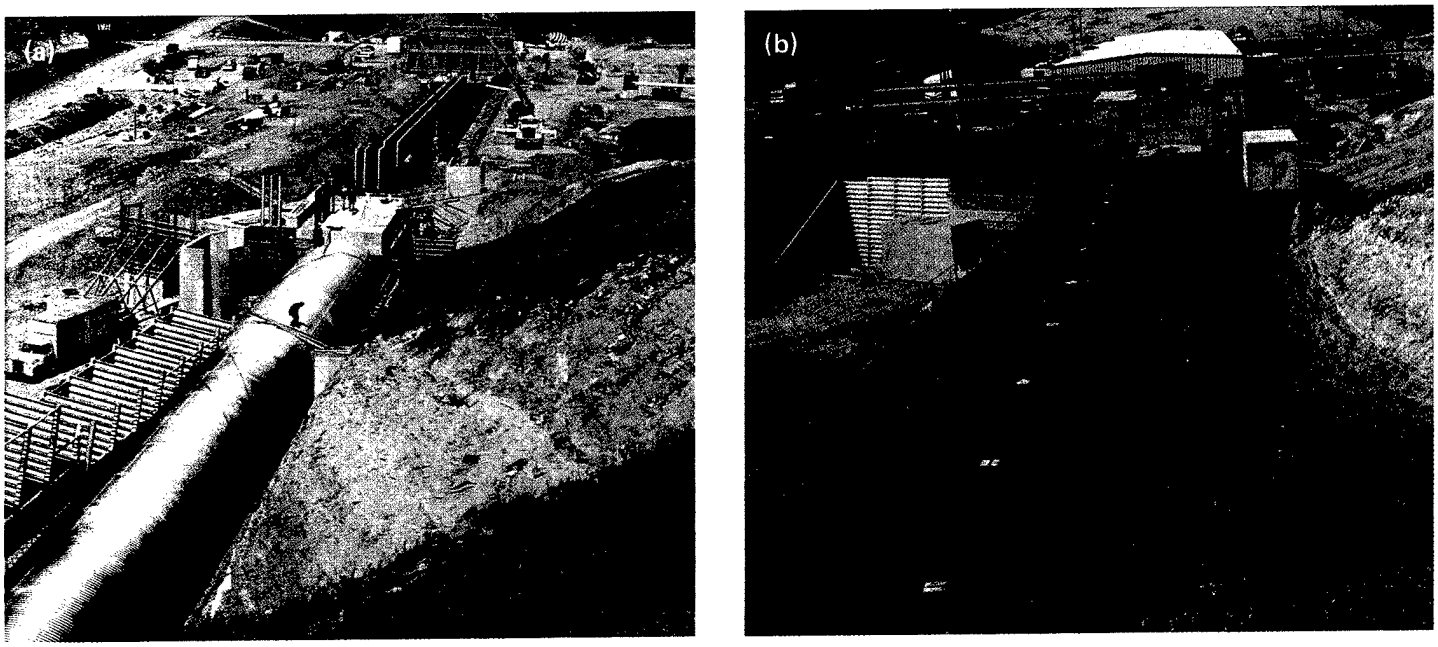

beams have attracted considerable interest in the scientific and defense communities. The military application that has received the most public attention is the use of intense beams of charged particles as point-defense weapons.

If it proves feasible to propagate charged-particle beams, their first use as weapons will be largely against targets within a few kilometres or less. Since they are so lethal, charged-particle beams can be used at distances too close to allow time for the "second shot" that might be necessary with less effective weapons. Early uses of the beams might be to defend large ships from cruise missiles[2] or for the close-range defense of hardened sites such as missile silos or national command authority centers. Such missions are called "point-defense" missions in distinction to area-defense missions.

Although the beam must bore its way through the air to the target, this process takes at most a few thousandths of a second. The deposition of megajoules of energy in the target is almost instantaneous. Therefore, beam weapons have the potential for engaging tens of targets per second, depending upon certain constraints in the system that controls their firing. These characteristics make beam weapons particularly well suited for countering small, very fast, highly maneuverable threats.

Accelerators have the demonstrated capability to convert upward of 30% of their prime electrical power into beam energy. If the electricity is produced with conventional generators powered with jet fuel, megajoules of beam energy can be produced with the consumption of approximately 10 litres of fuel. Consequently, even modest fuel supplies translate into a very large reserve of "ammunition" for a particle-beam weapon. This reserve makes it extremely difficult to overwhelm the particle beam with a large number of incoming threats.

Upon striking a target, the beam penetrates deeply and deposits its energy in a long, narrow cone. The high-energy electrons in the beam can penetrate tens of centimetres of solid aluminum, making it very difficult to shield against them. Damage to the target is immediate and severe; it includes structural damage, destruction or disruption of electronics equipment (e.g., missile guidance systems), and nearly instantaneous detonation of chemical explosives. An example of the damage a charged-particle beam of small radius can inflict on a target is shown in Fig. 2.

Not all the energy in a pulse reaches the target; some of it is lost in the atmosphere at a rate roughly proportional to the density of the air. Under normal conditions, the pulse will lose half its energy after traveling about 200 m. However, this loss rate does not limit the beam's range as much as might be expected. Much of the energy lost from the pulse goes into heating the air along the path of the beam. In a few microseconds, this hot air expands, leaving a channel of much lower density that the next pulse can follow with minimal energy loss. The use of bolts consisting of strings of pulses may allow propagation over long distances.

The electrons in the pulses scatter as they pass though the air, and the beam gradually widens. Because this spreading reduces the beam's power density on the target, the beam is useless as a weapon unless the spreading is inhibited. The large currents in the beam wrap it in a strong magnetic field (proportional to the current) that limits spreading by pinching the electrons closer together. This self-focusing occurs only when a high-current

Fig. 2

An example of the damage charged-particle beams can inflict. This aluminum disk (1 cm thick and 16 cm in diameter) was hit by an electron beam with about the same energy content but one-fifth the particle energy of an ATA beam pulse. The beam penetrated about 0.6 cm into the disk, melting the metal. An intense shock wave traveled through the disk, ripping away chunks of metal when it reached the rear surface (shown in figure). Photograph courtesy of Air Force Weapons Laboratory, Kirtland Air Force Base, New Mexico.

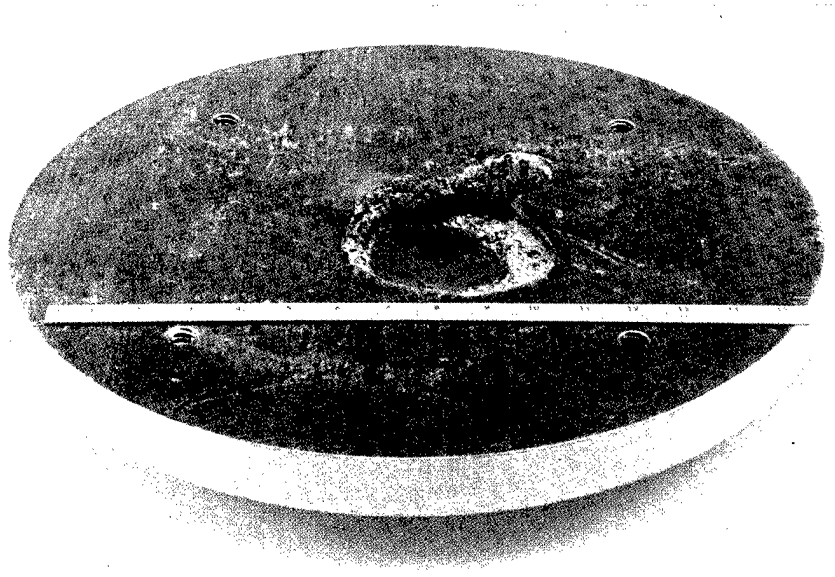

Table 1 Comparison of ATA with earlier induction accelerators.

	Astron II[a]	ERA[b]	ETA[c]	ATA[d]
Beam energy, MeV	6	4	4.5	50
Current, kA	0.8	1.2	10	10
Pulse length, ns	300	30	40	70
Burst rate, Hz	800	2	1000	1000
Average rate, Hz	5	2	5	5

[a] Lawrence Livermore National Laboratory, about 1968–1976.
[b] Electron Ring Accelerator (Lawrence Berkeley Laboratory).
[c] Experimental Test Accelerator (Lawrence Livermore National Laboratory).
[d] Advanced Test Accelerator (Lawrence Livermore National Laboratory).

beam is traveling through the air or some other gas. Self-focusing keeps the beam diameter down to a centimetre or so in air. When the focused beam hits the target, it deposits large quantities of energy in a small volume. The high-energy density makes the beam lethal.

The ATA's Role in Particle-Beam Research

The particle energy in a beam weapon determines how deeply the beam will penetrate the target. Although the ATA's energy level of 50 MeV will not cause beam penetrations as deep as more energetic beam weapons would, the ATA should provide data applicable to the designing of beam weapons. The ATA should enable us also to measure the radiation cone that extends far from the beam itself. (This radiation cone can cause significant damage to electronics equipment, thus increasing the effective range of a particle-beam weapon.) In both cases, scaling laws must be applied if we extrapolate our data to particle-beam weapons. Regardless of how our findings finally are applied, many complex weaponization issues will arise in the transition from the ATA to beam weapons.

Even though the particle energies of the ATA facility are well below those projected for beam weapons, we should be able, with high confidence, to extrapolate positive test results to increased energies. This close programmatic link between theory and experiment makes the ATA a cost-effective means for studying the physics of particle-beam weapons.

The ATA represents several large advances in high-intensity accelerator technology. The beam characteristics projected for the ATA (10-kA current, 50-MeV particle energy, 70-ns FWHM pulse, and 1-kHz repetition rate) are far beyond the capabilities of any existing accelerator. Table 1 compares the parameters of the ATA with those of the Astron II, the ETA, and the Lawrence Berkeley Laboratory's electron ring accelerator (ERA) injector.

In our experiments, we would like to test charged-particle beams over as wide a range of physical parameters as possible. The advantages to be gained from such exhaustive testing must, of course, be weighed against both the costs and the physical limits of the accelerator.

The ATA will enable us to determine the conditions under which stable and controllable beams can be propagated in open air. We can also test the beam's capability for inflicting damage and the performance of the nozzles that steer or aim it. As part of our effort to design a system for pointing and tracking, we will measure the degree to which microwaves or optical means can detect the beam path.

The particle energy of the ATA will be ten times that produced by the ETA. This increased particle energy means the ATA will have an order of magnitude more accelerator modules than the ETA, placing great demands on hardware reliability. The large number of components also makes it necessary to keep accelerator instabilities in mind when designing the beam-transport unit,

because the focusing requirements are unusually stringent.

To ensure this high level of component reliability, we are using the ETA to test ATA technology on a small scale. The ETA will be used to verify the projected performance levels of the electron source, the 1-kHz pulsed-power components, and the beam-control system for the ATA. Since its initial operation in mid-1979, the ETA has achieved all design goals and has produced several million beam pulses. The ETA, therefore, has provided the necessary data base for design of high-voltage components for the ATA, which will produce a few million beam pulses per year in normal operation.

The ATA Design

The 200-m ATA Facility has an 85-m linear electron accelerator and consists of four major units: a pulse-forming network, an electron injector, a series of accelerator modules, and an experiment tank (see Fig. 3). The pulse-forming network provides short, high-voltage pulses that power the electron injector and accelerator modules. The injector produces a 10-kA beam of 2.5-MeV electrons, which are guided by magnetic

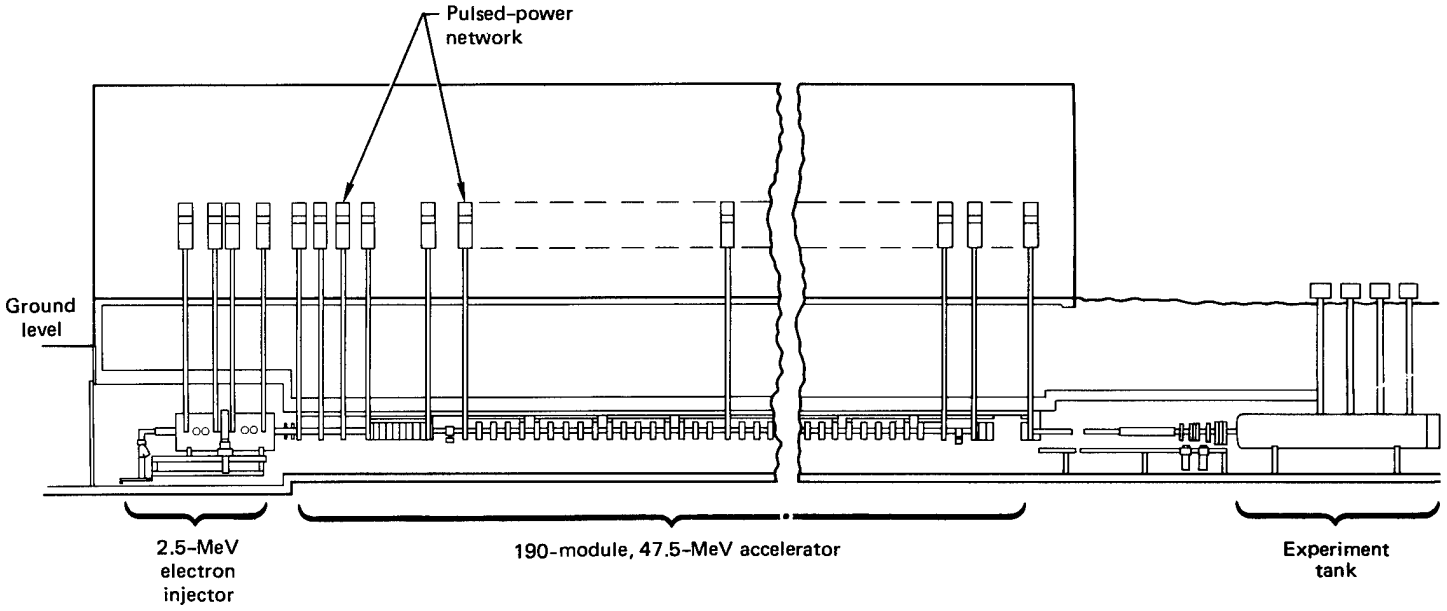

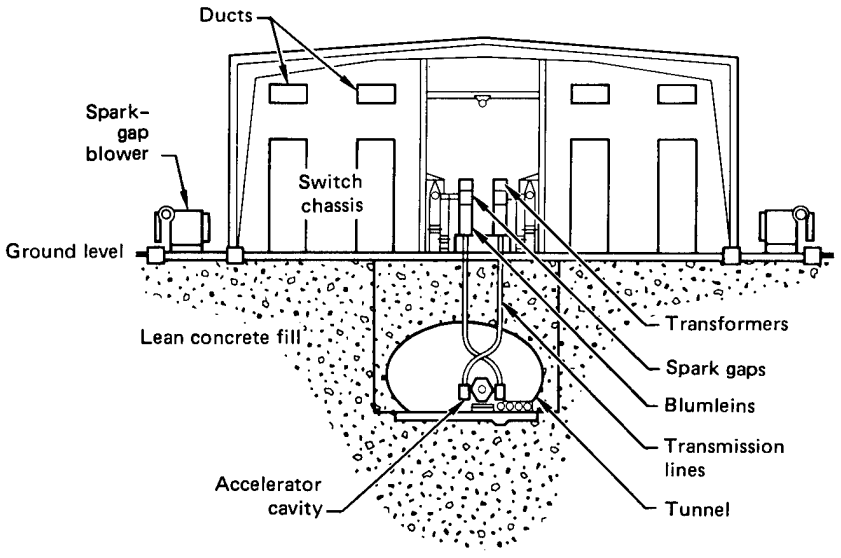

Fig. 3

Sketch of the ATA facility showing arrangement of major components: the pulsed-power network, the electron injector, the accelerator, and the shielded, gas-filled experiment tank. (Many of the vertical elements forming the pulsed-power network have been omitted for simplicity.) This whole assemblage will be 200 m long. The cross-section of the accelerator shows the end of one accelerator cavity, located in an underground tunnel, as well as the Blumleins connecting it to the pulsed-power transformers above ground.

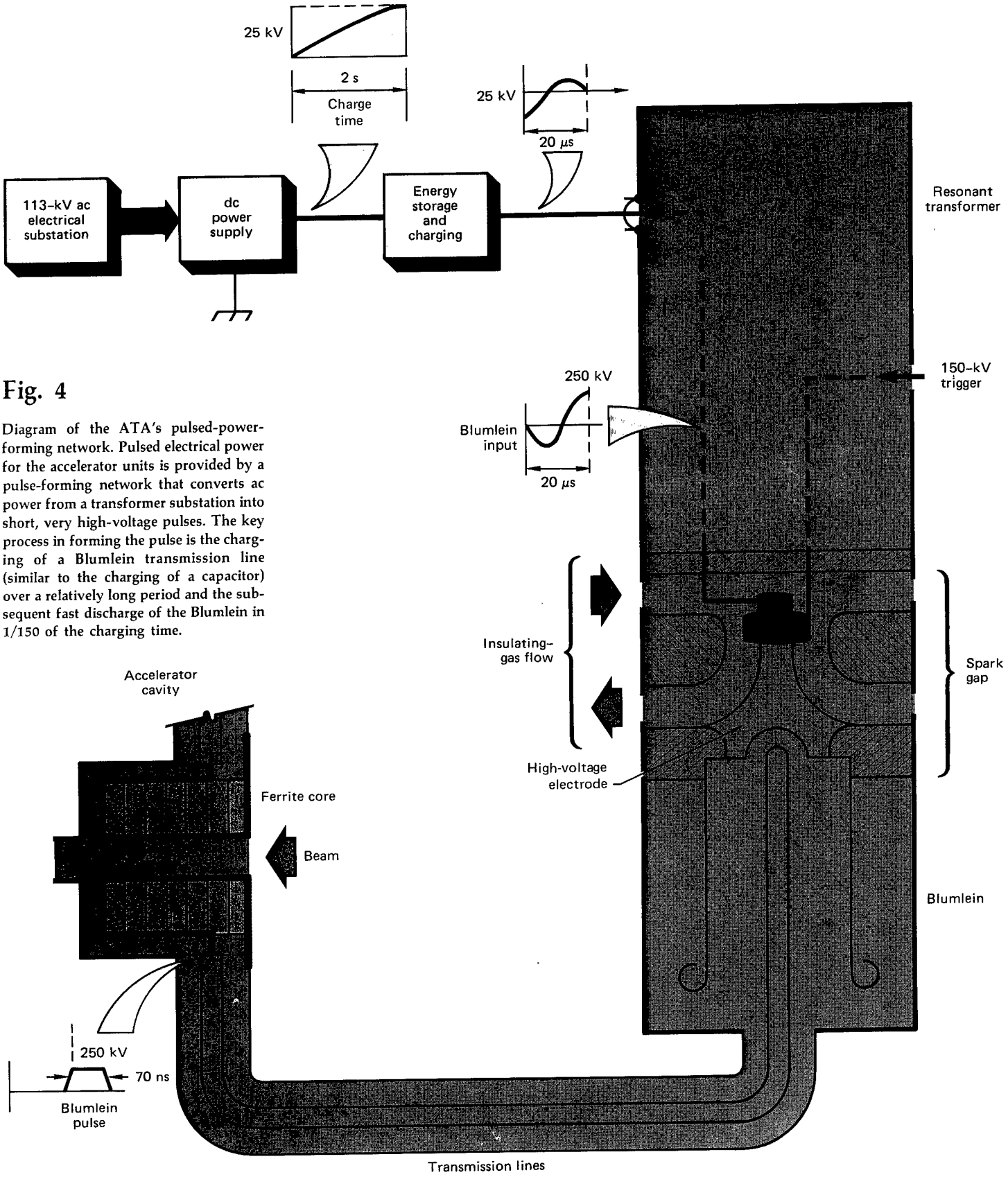

Fig. 4

Diagram of the ATA's pulsed-power-forming network. Pulsed electrical power for the accelerator units is provided by a pulse-forming network that converts ac power from a transformer substation into short, very high-voltage pulses. The key process in forming the pulse is the charging of a Blumlein transmission line (similar to the charging of a capacitor) over a relatively long period and the subsequent fast discharge of the Blumlein in 1/150 of the charging time.

fields through an accelerator consisting of 190 separate accelerator modules (cavities). The accelerator increases the electron energy to 50 MeV in 190 separate increments of 0.25 MeV. When they are at full energy, the electrons, still guided by magnetic fields, pass into an experiment tank that contains gas of variable type and pressure and that is covered with a thick layer of earth and concrete to absorb any stray radiation.

Pulsed-Power Network

The pulsed electrical power is provided by a pulse-forming network (Fig. 4) that stores a discrete amount of energy over a period of time in order to compress it and then suddenly releases it as a pulse. The power is stored in components such as an electrical transmission line that is charged to a desired voltage in much the same manner as a capacitor. A transmission line (Blumlein) composed of three concentric, metal conducting cylinders is frequently used in pulsed-electron accelerators.

Figure 4 shows how energy is converted to the beam from primary ac power. The ac power drives a high-voltage dc power supply which, in turn, feeds an energy storage and charging network. The pulse from this network is stepped up to 250 kV by a resonant transformer bolted to the Blumlein transmission line. When the current that has charged the Blumlein drops to zero, a spark-gap switch (filled with gas at high pressure) is fired by a 150-kV trigger circuit. The resulting high-voltage discharge from the Blumlein is then impressed across the accelerating gap. As long as this pulse persists, electrons passing by the gap will be accelerated. The energy stored in the Blumlein in 10 μs is delivered to the acceleration cavity in 70 ns, almost 150 times faster.

The Blumlein can be recharged (by having an insulating gas flow through the spark-gap switch at high velocity) and then fired again at a 1-kHz burst rate. The voltage-holding ability of this switch (developed for ATA) determines the maximum accelerating voltage per ATA module. Because of limitations in the energy-storage subsystem, the spark gap is fired in bursts of ten consecutive pulses with two-second rests between bursts.

Electron Injector

The source of the high-current electron beam is the electron injector, or gun. The ATA's 2.5-MeV electron injector, the second major unit in the accelerator, is typical of the pulsed-power technology used throughout the system. Acceleration voltages in both the electron injector and the accelerator module are generated by similar power-supply and pulse-forming networks feeding the ferrite induction cores.

Our coordinated program of theory and experiments with the ATA has the goal of providing a complete understanding of beam-propagation physics.

The 10-kA current produced by the injector requires special design features to control the defocusing effects of the electromagnetic fields the beam itself generates. These fields lead to a net force that is the difference between the electrostatic self-repulsion of the electron cluster and the magnetic pinch forces that tend to hold the beam together. For beams with kinetic energy greater than their rest mass energy, these forces nearly cancel

(the net repulsive force is proportional to the inverse square of the beam energy).

Figure 5 is a schematic cross section of the ATA's electron injector. Here (as in a conventional vacuum tube) a high-voltage pulse is applied to a grid to extract the required current from the cathode. In the vicinity of the grid, the repulsive self-fields of the beam are shorted by the grid; this causes an initial focusing of the beam (as Fig. 5 shows). When the grid pulses, the anode is pulsed simultaneously to 2.5 MV, rapidly raising the kinetic energy of the electrons as they traverse the region between the grid and anode. Although the defocusing forces are reduced by the increase in beam energy, solenoidal coils are needed to control and focus the beam for transport through the accelerator module.

The electron injector is constructed in two parts, each with five 0.25-MV induction units in series to provide the 2.5-MV anode/cathode voltage pulse. This voltage also appears across two large ceramic accelerator columns that are divided by metallic rings into ten segments. The segments are connected by power resistors to ensure proper voltage distribution across the column to avoid electrical breakdown. The accelerator columns also serve as the barrier between the vacuum in the beam area and the dielectric oil that fills the induction units. The division of the injector into two parts has several advantages: it provides a vacuum pumping port in the center of the injector, partially shields its ceramic insulators from the electron beam, and makes assembly easier.

The Accelerator Module

The accelerator module is the heart of a multistage accelerator like the ATA. Each accelerator module adds an incremental kinetic energy to the beam. Therefore, by increasing the number of modules that make up the accelerator, one can increase the beam energy to any desired level. In a qualitative sense, the linear induction accelerator is just a series of one-to-one pulse transformers. The primary circuit

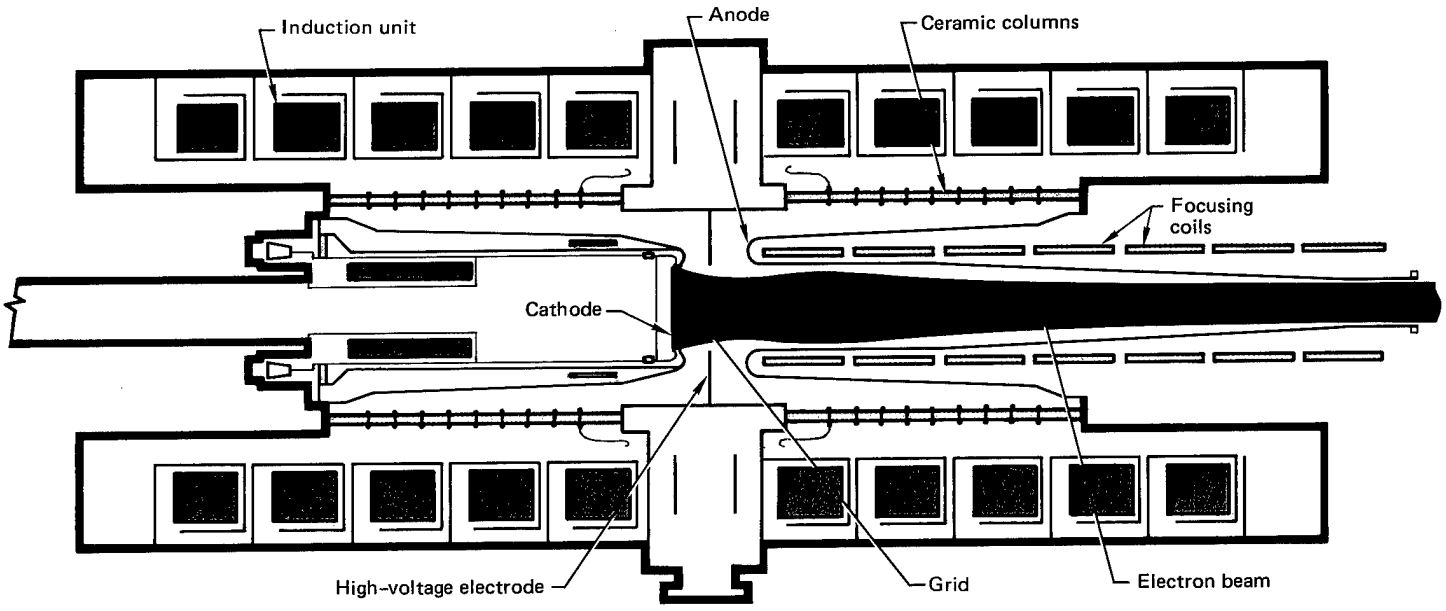

Fig. 5

A schematic drawing of the 2.5-MeV electron injector for the ATA. The 2.5 MV between the anode and cathode (provided by 10 induction accelerator units of 0.25 MV each, connected in series) extracts 10 kA from the large cathode. Note that the beam begins to spread soon after it enters the anode but that focusing coils quickly focus it to a smaller diameter before it is injected into the accelerator. The beam's spreading and focusing is drawn here according to precise calculations of actual beam behavior.

of the transformer is the pulse-forming network previously described. The secondary circuit of the transformer is the electron beam itself. As Fig. 6a illustrates, the primary circuit loops around the magnetic core once, just as the electron beam threads through each core once. In such a transformer, the voltage induced in the secondary circuit is just that in the primary circuit.

The acceleration process can be described more specifically (Fig. 6b). Before the beam enters each cavity, the ferromagnetic cores are magnetized (set) to a maximum magnetic field. Then, a voltage pulse from the coaxial transmission line is impressed upon the acceleration gap. The ferrite torus acts as an inductance, initially preventing a large current from flowing through the structure around the ferrite, thereby keeping the coaxial line from shorting. In accord with the law of magnetic induction, this current increases at a steady rate given by the ratio of the voltage pulse to the ferrite inductance. In addition, the magnetic field in the core decreases from its initial value at a constant rate until the field attains a minimum value. At this time, the applied voltage pulse ends. In addition to the time-varying fields that accelerate the electron cluster, there are static magnetic fields that guide the beam as it moves down the accelerator from one cavity to

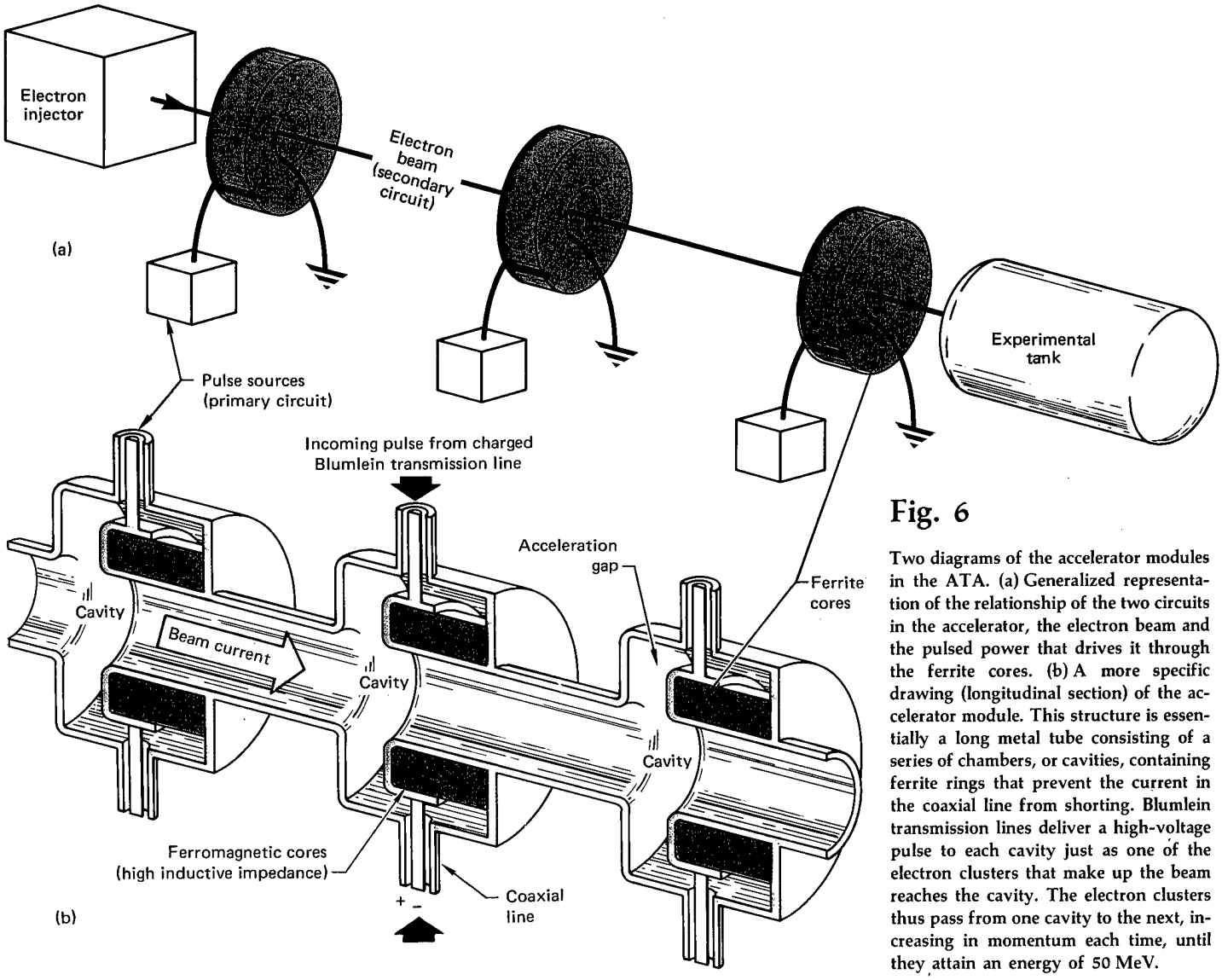

Fig. 6

Two diagrams of the accelerator modules in the ATA. (a) Generalized representation of the relationship of the two circuits in the accelerator, the electron beam and the pulsed power that drives it through the ferrite cores. (b) A more specific drawing (longitudinal section) of the accelerator module. This structure is essentially a long metal tube consisting of a series of chambers, or cavities, containing ferrite rings that prevent the current in the coaxial line from shorting. Blumlein transmission lines deliver a high-voltage pulse to each cavity just as one of the electron clusters that make up the beam reaches the cavity. The electron clusters thus pass from one cavity to the next, increasing in momentum each time, until they attain an energy of 50 MeV.

the next. A model of a section of the accelerator is shown in Fig. 7.

In induction accelerators, it is important that the voltage pulse to the acceleration cavity coincide with the arrival of one of the electron clusters that are passing through the accelerator module. Proper timing is ensured by appropriate delays in the triggering circuits of the pulsed-power network.

An important complication in any electron accelerator is that the traveling electron clusters generate electromagnetic fields that are modified by the accelerator structure. This coupling can distort the accelerating fields and limit the output current. It can also cause small, random perturbations in the beam's position or structure that lead to damaging or current-limiting instabilities. Because the beam fields increase with the beam current, these perturbations are especially serious in high-current accelerators. Furthermore, the current-limiting

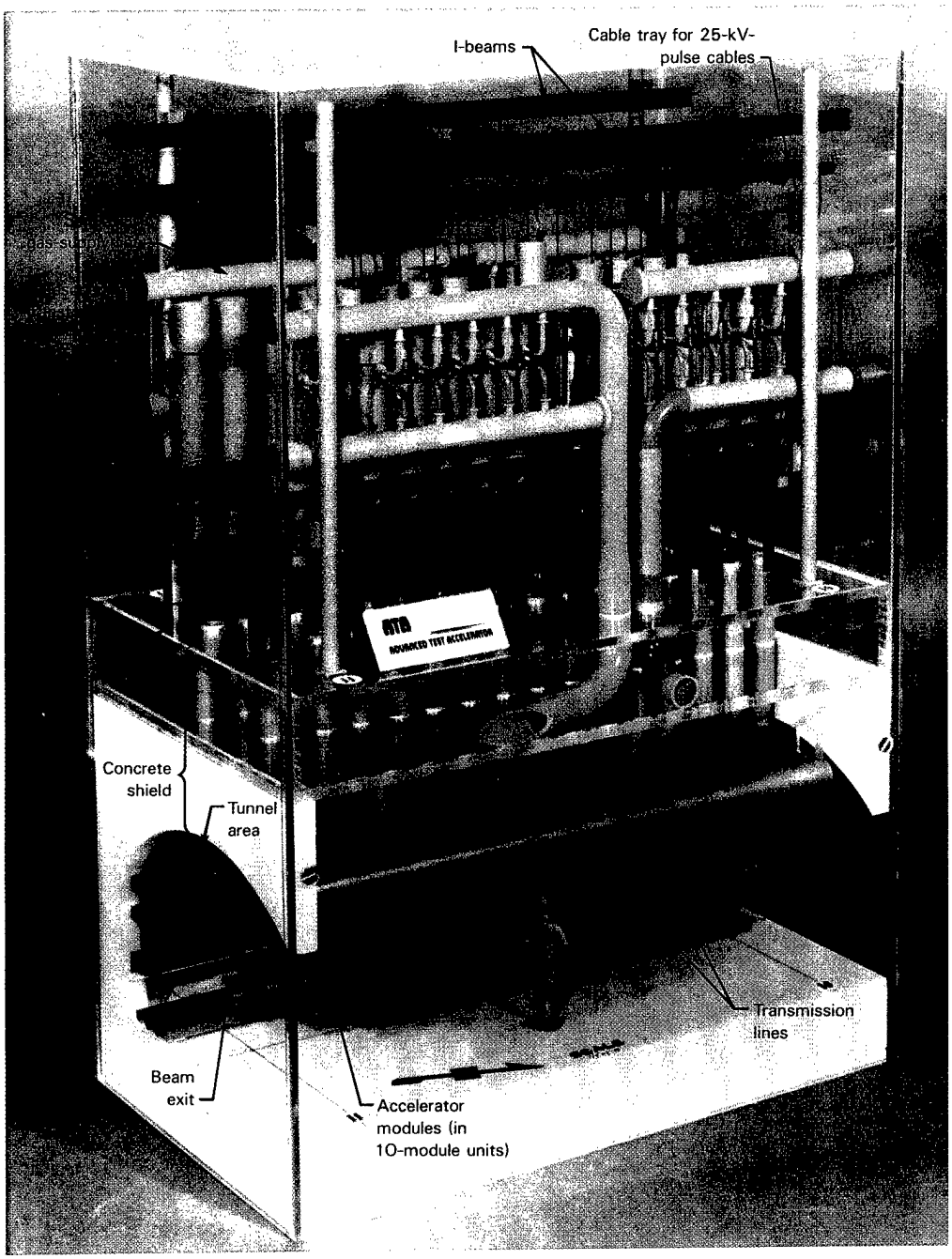

Fig. 7

Model of a section of the ATA's accelerator and its pulse-forming power supply. This model represents a structure approximately 16 m high. The components below ground level are embedded in a concrete arch over the tunnel area. The components above ground can be raised for inspection by means of a crane attached to the I-beams.

instabilities grow exponentially with the number of accelerator cavities. The unusually high beam current of the ATA and the ETA necessitates the choice of high-voltage accelerator modules with toroidal ferrite cores rather than lower-voltage, soft iron units such as were used on the Astron. This choice reduces the number of accelerator structures that can interact with the electron beam, suppressing potential instabilities.

Experimental Facility

Once the electrons have acquired their final energy, 50 MeV, they are guided by a series of steering and focusing magnets into a large tank that can be filled with gas of various composition and pressure. This tank is located in an 80-m-long underground tunnel (Fig. 8).

The first experiments to be performed after the accelerator construction is completed will be measurements of beam current and voltage waveform and their variation on a pulse-to-pulse basis. We will measure also the spatial distribution and angular divergence of the beam. When we understand the nature of the beam and its pulse-to-pulse reproducibility, we will begin studies of beam stability and dynamics as well as beam interactions with gas and plasma.

For all such studies, we require accurate measurements. Line-of-sight holes from the ground surface into the tunnel provide a means of removing sensitive diagnostic equipment from the intense radiation environment the ATA beam will produce. A diagnostic bunker near the entrance to the tunnel will accommodate the fast diagnostics needed to study the physics of beam/gas interactions. Both the diagnostics for beam/gas interaction studies and the specially designed voltage and current probes will be monitored by the ATA control system to provide accurate and complete records of all experiments.

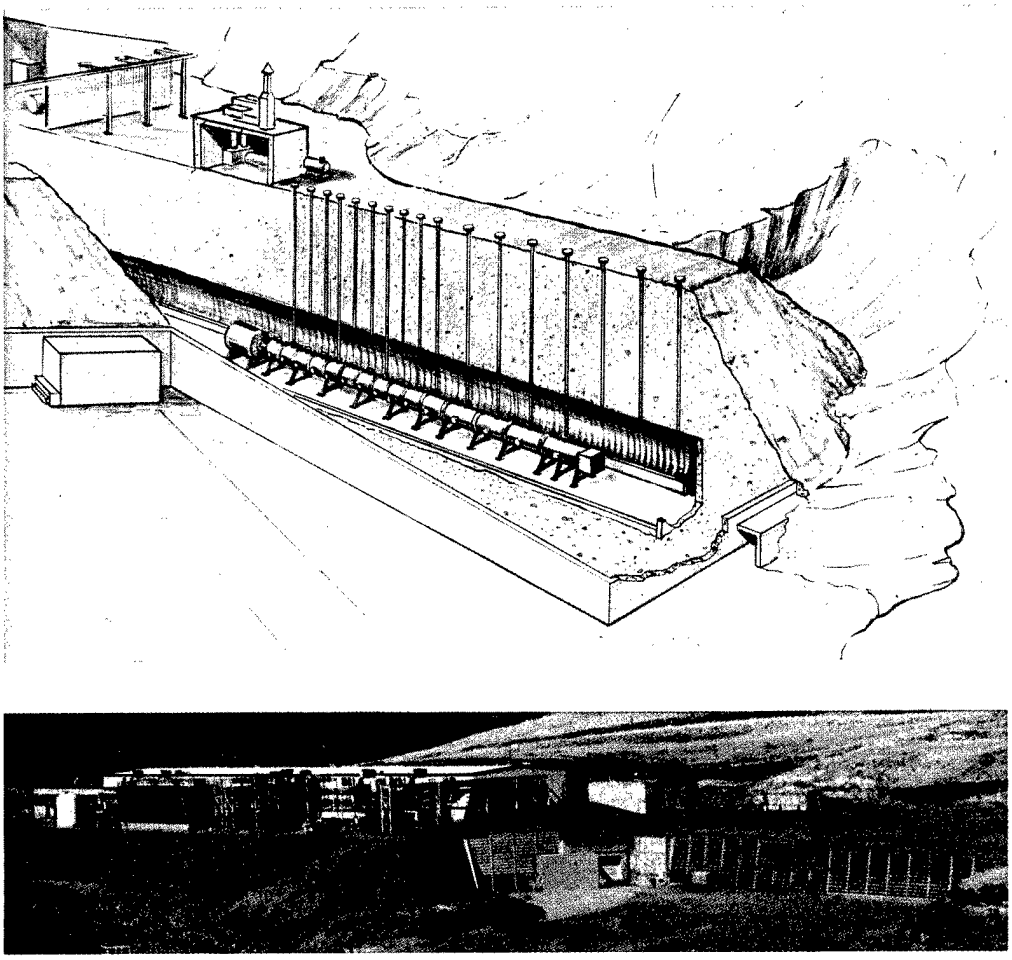

Fig. 8

The completed ATA facility will permit experiments on beam behavior both in a shielded gas tank and in open air. The artist's sketch shows the underground experiment tank into which the beam will be directed. The thick earth cover will absorb stray radiation, and the pipes from the ground surface down to the tunnel will allow access for diagnostic instruments. The instruments can be monitored from the shielded bunker above the tank. To the left of the tank, a door can be opened to allow the beam to be aimed into the atmosphere. In the photograph (taken in October 1981), the concrete door has been rolled aside.

Conclusion

Our coordinated program of theory and experiments with the ATA has the goal of providing a complete understanding of beam-propagation physics. Our DARPA-funded program in particle-beam technology has yielded a body of knowledge about high-intensity accelerators and beam physics that we can build upon with the ATA. We expect to obtain high-quality, high-current electron beams with energies at least an order of magnitude greater than any other repetition-rated accelerator has produced. The ATA promises advances in high-intensity accelerator technology that are essential to a wide range of applications, including beam weapons.

Key Words: accelerator; advanced test accelerator; ATA; charged-particle-beam weapon; electron accelerator; electron-beam propagation; experimental test accelerator; ETA; linear accelerator; particle beam.

Notes and References

1. For information on the dedication of the Advanced Test Accelerator, see *Energy and Technology Review* (UCRL 52000-81-1), January 1981, p. ii.
2. W. E. Wright, "Charged Particle Beams. Could We? Should We?," *Proceedings of the U.S. Naval Institute*, U.S. Naval Institute Press, Annapolis, MD (November 1979).

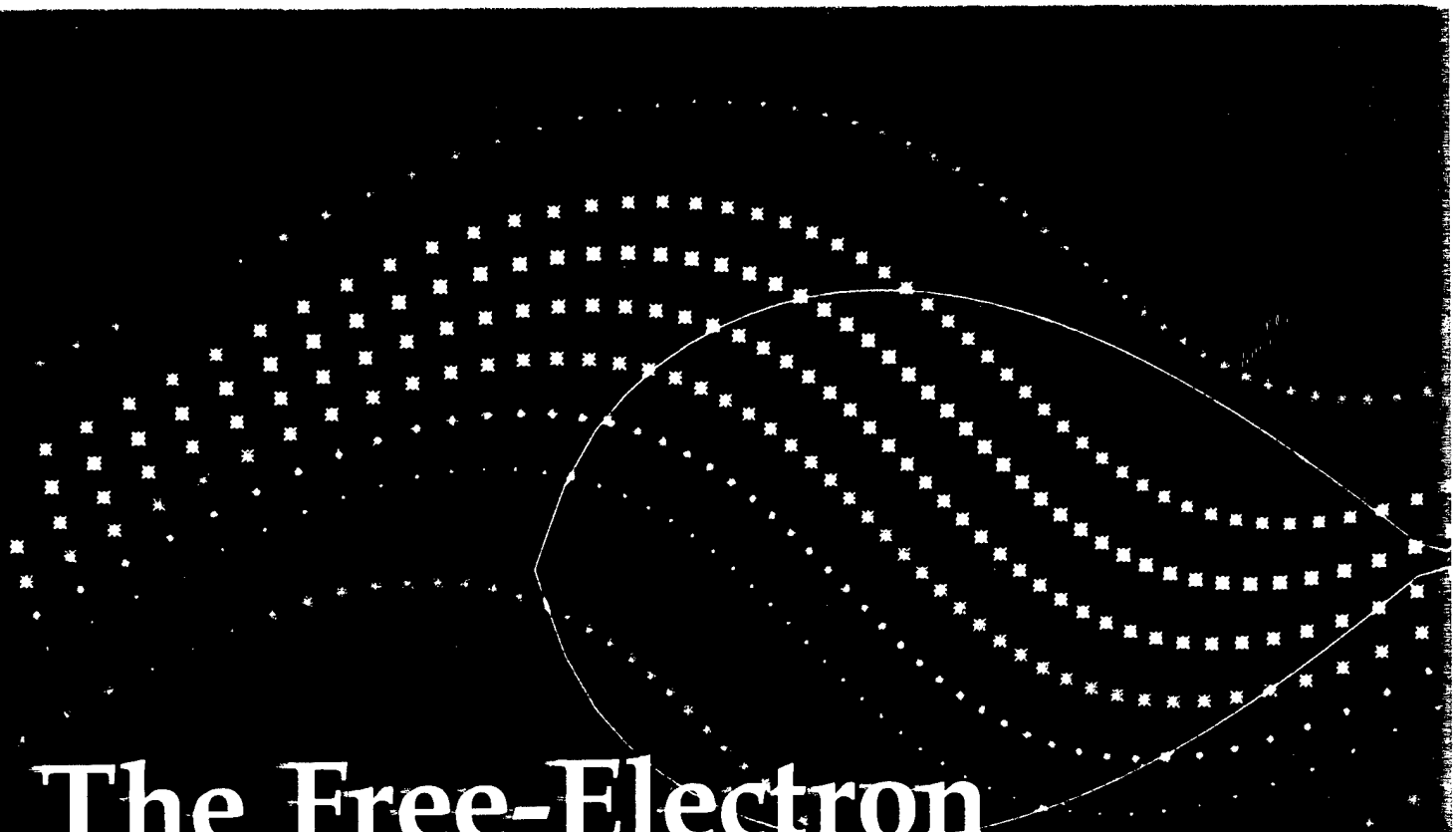

The Free-Electron Laser Amplifier

Recent experiments have shown that the energy in a high-quality electron beam can be directly converted to laser radiation; analysis suggests that this process may be suitably efficient and scalable in power for use in the production of power by inertial confinement fusion. We are conducting computer simulation studies of the conversion process.

The manifold and expanding applications of laser technology now include optical communications, photochemistry, weapon systems, and inertial confinement fusion (ICF) research. Many of these applications require an intense, highly efficient source of laser radiation. In conventional lasers, population inversions between characteristic states of a solid, liquid, or gaseous medium are created by various means of excitation such as electrical discharge or chemical or optical pumping. The excitation energy is then extracted as coherent light. As these energy transformation processes usually entail unavoidable losses. they

For further information contact Donald Prosnitz (415) 422-7504 or James C. Swingle (415) 422-7188.

impose limits on the efficiency and power capability of such lasers. One way to bypass these problems is to convert electrical energy directly to coherent radiation.

A promising technology for direct energy conversion, still in the exploratory stage, is the free-electron laser (FEL). The FEL operates on principles radically different from those of conventional lasers by directly converting kinetic energy in a high-energy (relativistic) electron beam into coherent radiant energy.[1]

Direct conversion already has produced coherent radiation in the longer-wavelength (radio wave and microwave) regions of the electromagnetic spectrum. Figure 1 shows the efficiency of converting electron-beam energy into radiation in electromagnetic generators of various types. Long-wavelength radiation is now produced with very high (70%) efficiency by radio tubes, gyrocons, and klystrons. Gyrocons and traveling-wave tubes have demonstrated efficiencies of 20% to 60% in the microwave region, with even higher efficiencies projected. The FEL is the short-wavelength analogue of these devices.

We are doing computer-simulation studies of the FEL to investigate its potential for increasing the power output of conventional lasers. Should electron-beam accelerators with the appropriate characteristics prove feasible, we envision FEL systems capable of efficiently generating high-power coherent radiation spanning the spectral region from the far infrared to the ultraviolet. Our studies of the FEL suggest that, in the shorter-wavelength region from 10 to 10^{-1} μm, conversion efficiencies approaching 30% may be achievable.

The development of low-cost and efficient short-pulse lasers in the ultraviolet and visible regions is a technology of particular interest in ICF research. Most current FEL research is sponsored by the Department of Defense and centers on the use of radiofrequency linear accelerators more suited to applications requiring low peak power and high average power. In the Laboratory's Laser Fusion Program, we are examining the use of FELs based on linear induction accelerators producing high peak power as a driver for inertial confinement fusion reactors.

ICF research at LLNL[2] has reached the point where we can estimate performance specifications for an ICF reactor capable of generating power on a commercial scale. The production of economically competitive ICF power requires, among other things, the availability of a

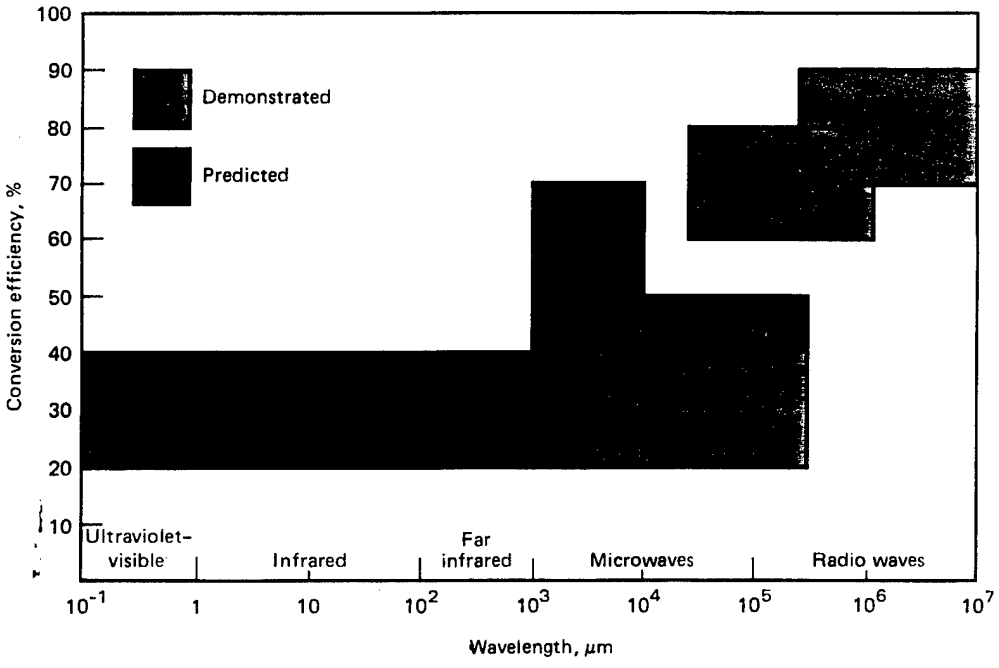

Fig. 1

Efficiency of electromagnetic generators of various types in converting electron-beam energy to radiation. The conversion efficiencies shown are for an electron beam alone; overall system efficiency for an FEL would be somewhat lower (10 to 20%).

relatively inexpensive (≤$100/J) and efficient (≤10%) driver capable of delivering a several megajoule pulse of 10- to 20-ns duration to a target one-half centimetre in diameter several times per second.

Although conventional lasers eventually may reach such performance levels, at present they are relatively inefficient (1% to 10% conversion efficiency) and expensive ($300 per optical joule). More efficient methods of energy conversion are needed to close the present gap between laboratory devices and commercial power applications. Our studies suggest that the FEL may attain conversion efficiencies of 15% to 20% at a cost of $100 per optical joule.

Mechanism of Energy Conversion

The basic operating principle of the FEL is to amplify the intensity of a propagating laser field by using the radiation emitted from high-energy electrons. Consider, for simplicity, the case of a single electron. To directly convert the kinetic energy of an electron to radiation, it is necessary to perturb the electron's motion. This can be done by passing it through a magnetic field that is static in time but periodic (alternating) in space. An electron entering such a field acquires a transverse oscillatory motion (Fig. 2). In the FEL, the field is produced by a series of magnets called a "wiggler."

A laser beam entering the wiggler from the same direction as the electron is polarized so that the electrical component of the laser's radiation field acts to retard the electron's oscillatory motion (see box on p. 22). The kinetic energy lost by the electron (in the form of radiation) as it decelerates is transferred to the laser's radiation field. The net result is that the electron is traveling a little slower at the output end of the device than when it entered, and the intensity of the laser field has been amplified.

To achieve a net transfer of energy from an electron to the laser field, it is necessary to maintain a precise relationship among the velocity of the electron, the spacing (or period) and strength of the wiggler magnetic field, and the wavelength of the laser field. This is called the synchronism condition. At nonrelativistic electron energies, this condition specifies that the spacing of the wiggler field must be approximately the same as the wavelength of the laser field. By designing the wiggler spacing and adjusting the electron velocity appropriately, we can cause electrons to radiate at the frequency of the laser field.

However, because of the technical difficulty of fabricating very small magnets, the radiation that can be amplified at nonrelativistic electron energies is limited to wavelengths longer than several millimetres, considerably greater than those necessary with laser fusion devices. The problem, then, is to find a technique for generating radiation at the requisite wavelengths within the contraint imposed by magnet size.

This problem can be solved by giving the electron an initial velocity high enough so that relativistic effects become important. Two effects predicted by the special theory of relativity come into play at this point. One is the Lorentz contraction (see box on p. 28). This effect causes the spacing of the magnetic field to appear much shorter (contract) in the frame of reference of an electron moving through the wiggler. Simultaneously, in the laboratory's frame of reference, the wavelength of radiation emitted by the electron undergoes a relativistic Doppler shift, causing it to appear shorter. With careful adjustment of the electron's initial velocity, the electron will emit radiation at a wavelength corresponding to the

Fig. 2

Mechanism of energy transfer in the FEL. An electron is injected (in the z direction) into the field, B_w, of a periodic array of magnets (the "wiggler"), which imposes a transverse oscillatory motion on the electron (in the y direction) as it traverses the array. This oscillatory motion causes the electron to emit electromagnetic radiation. The kinetic energy lost by the electron is transferred to a co-propagating electromagnetic (laser) field (E_s).

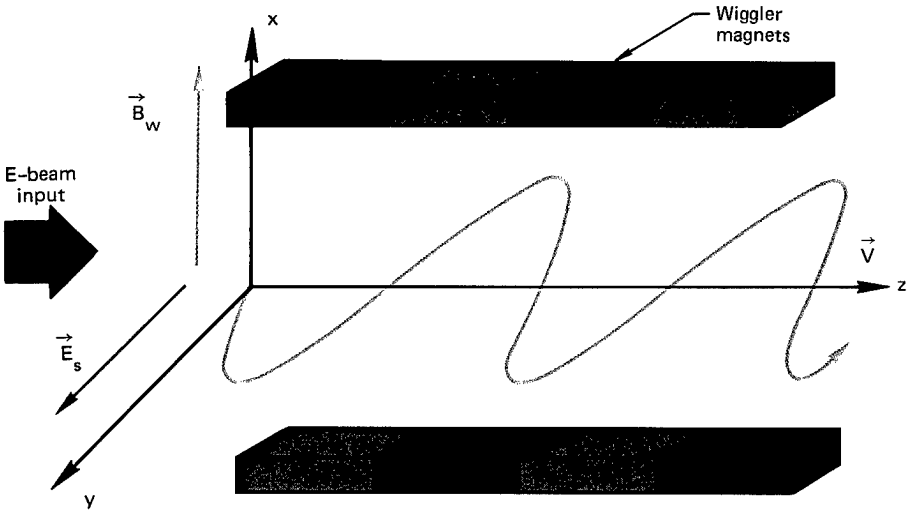

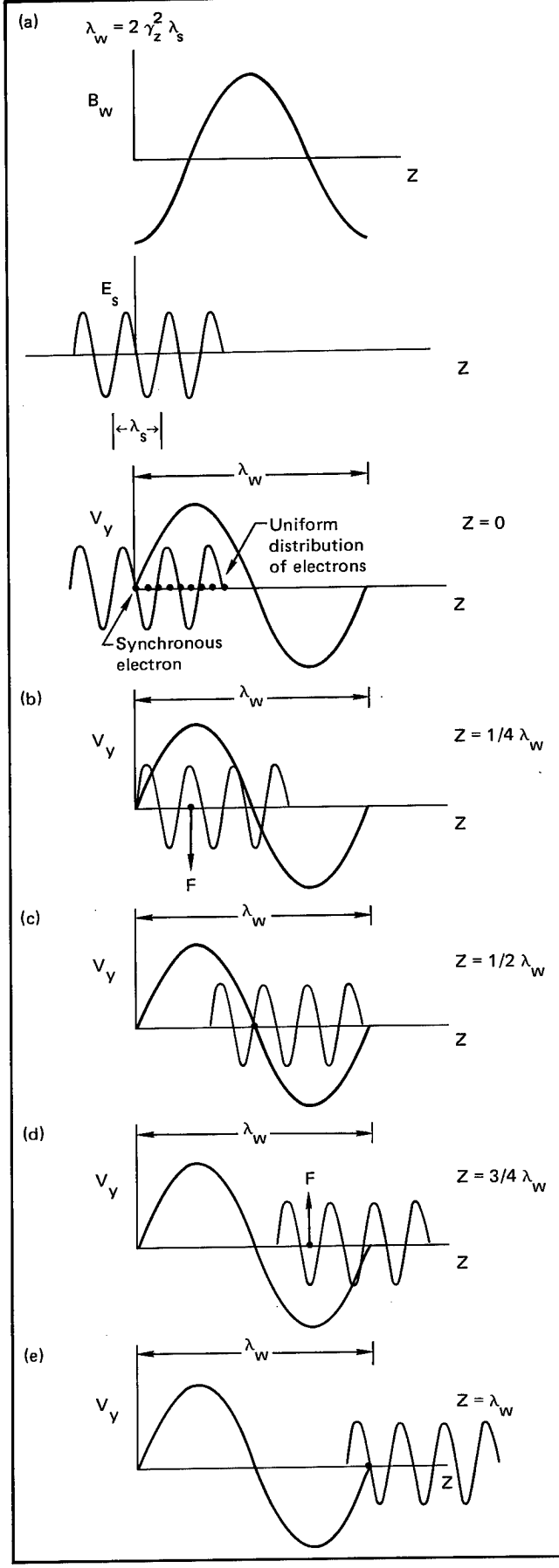

Deceleration of an Electron by an Electromagnetic Field

A laser beam entering the wiggler from the same direction as the electron is polarized so that the electrical component of the laser's radiation field acts to retard the electron's oscillatory motion. The kinetic energy lost by the electron (in the form of radiation) as it decelerates is transferred to the laser's radiation field. The net result is that the electron is traveling a little slower at the output end of the device than when it entered, and the intensity of the laser field has been amplified.

(a) The initial wiggler magnetic field, B_w, laser electric field, E_s, of wavelength λ_s, and velocity of the electron V_y. As the electric field at the position of the synchronous electron is zero, the laser's field does no work on the electron.

(b) The synchronous electron has now traveled 1/4 of a wiggler spacing, λ_w. The electric field and the electron's velocity are now both positively directed, so that the laser field exerts a decelerating force on the electron, effectively transferring energy from the electron to the laser field.

(c) The electron has traversed 1/2 of a wiggler spacing. The laser field seen by the electron is now zero, so that no net force is exerted on the electron.

(d) The electron has traversed 3/4 of a wiggler spacing. The laser field and the electron's velocity are now both negatively directed. Once again, a decelerating force acts on the electron, transferring energy from the electron to the laser field.

(e) The electron has now traveled one full wiggler spacing, and the situation is again as in (a). The laser field has traveled one wiggler spacing plus one laser wavelength while the electron has traveled one wiggler spacing. (This synchronism requires that $\lambda_s = \lambda_w/2\gamma_z^2$, as in the relativistic case; see box on p. 28) Net energy has been transferred from the electron to the laser field, and the cycle begins again.

wavelength of the laser field, thereby amplifying the intensity of the field.

The synchronism requirement raises an additional design issue. As an electron travels through the wiggler and loses energy, its velocity decreases. The design of the wiggler must be adjusted to ensure that the spacing of the wiggler field remains the same as the wavelength of the laser field in the electron's frame of reference. The solution is a variable (tapered) wiggler, whose magnetic-field-reversal spacing changes as a function of distance along its length.

Extension of the Concept to Many Electrons

Developments in accelerator technology must accompany development of the FEL. Important constraints are imposed on this technology when the FEL concept is extended from a single synchronous electron to the case of many electrons in an actual electron beam. At present, we are using computer simulations to estimate the efficiency with which energy can be extracted from an electron beam by the FEL amplifier.[3]

Although the synchronism condition described above applies well to monoenergetic electron beams that are tightly clustered in space, real beams will have initially a uniform distribution along the axis of the FEL. This suggests that many electrons will fail to satisfy the synchronism condition, seriously reducing the efficiency of energy extraction.

Fortunately, there is a mitigating mechanism. Recent studies indicate that if the laser (electromagnetic) field is quite strong, any electron with an energy close to the synchronous energy will, on the average, lose energy at the same rate as a synchronous electron.[4] The laser field, in effect, selects electrons with the proper phase relationship. Entire ensembles of electrons may then interact coherently with the laser field, permitting high energy-extraction efficiencies. Our simulation studies are designed to verify this phenomenon.

Our studies have predicted the dynamic behavior of a typical electron cluster in a FEL. Figure 3a shows initial energies and positions of a cluster of 500 electrons one optical wavelength long as

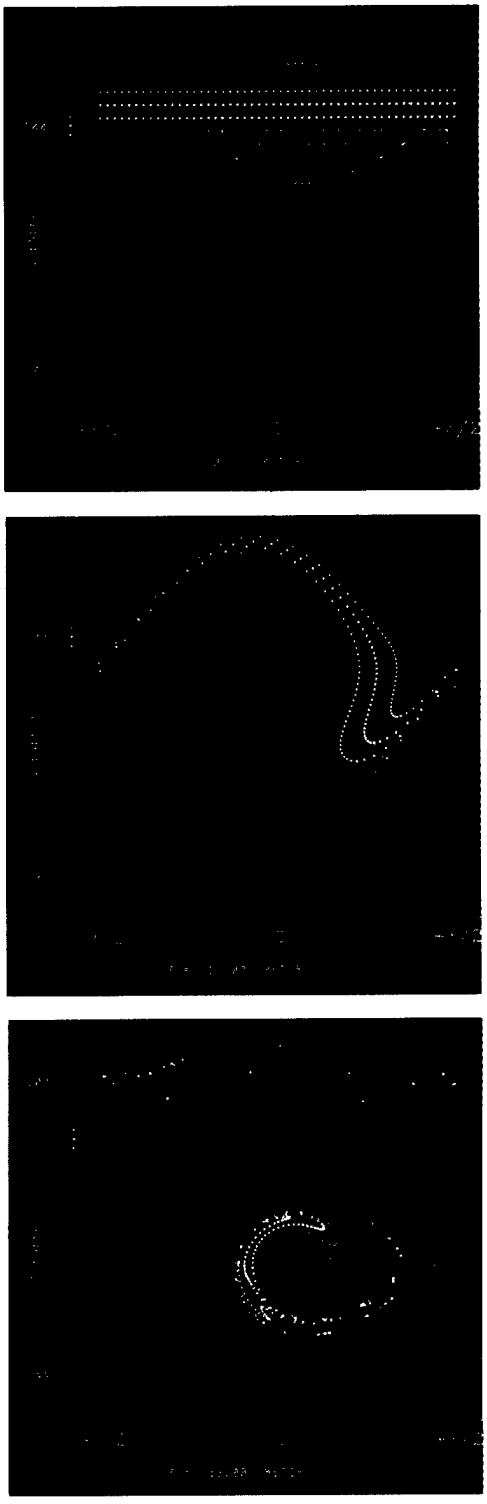

Fig. 3

(a) A cluster of 500 electrons one optical wavelength long as it enters the wiggler. The fish-shaped curve is called a "bucket." Electrons sufficiently close to the synchronous electron located at the center of the bucket lose energy at the same rate it does. (b) The same cluster of electrons after it has traveled 12 m down the wiggler. Some electrons have gained and others have lost energy; the net result is a minimal transfer of energy to the laser field. (c) 36 m down the wiggler, the electron cluster has divided; one cluster retains the initial energy and a second cluster has been trapped in the bucket and decelerated, thereby transferring large amounts of energy to the laser field.

it enters the wiggler. The fish-shaped curve surrounding most of the electrons is known as a "bucket." Our approximate calculations indicate that the electrons within the bucket should be close enough to the synchronous electron to lose energy at the same rate as it does. Figure 3b shows the same cluster of electrons after it has traveled 12 m down the wiggler. Some electrons have gained and others have lost energy; the net result at this point is a minimal transfer of energy to the laser field. In Fig. 3c, however, 36 m down the wiggler the electron cluster has divided. One cluster retains the initial energy and a second cluster has been trapped in the bucket and decelerated, thereby transferring large amounts of energy to the laser field.

Our one-dimensional model did not simulate the normal diffraction of the laser field or its refraction by the electron cluster. We are refining a two-dimensional model that will enable us to simulate propagation of the optical beam through the FEL and will include diffraction and refraction effects. Our preliminary results, shown in Fig. 4, suggest that the optical beam will propagate satisfactorily even if the wiggler is very long.

Designing a Fusion-Class FEL System

We have also used our one-dimensional model to simulate fusion-class FEL devices. The results indicate that high extraction energies can be most economically achieved if the laser operates at very high intensities (greater than 10 TW/cm^2). Such intensities would eliminate the need for final focusing optics—a source of significant energy

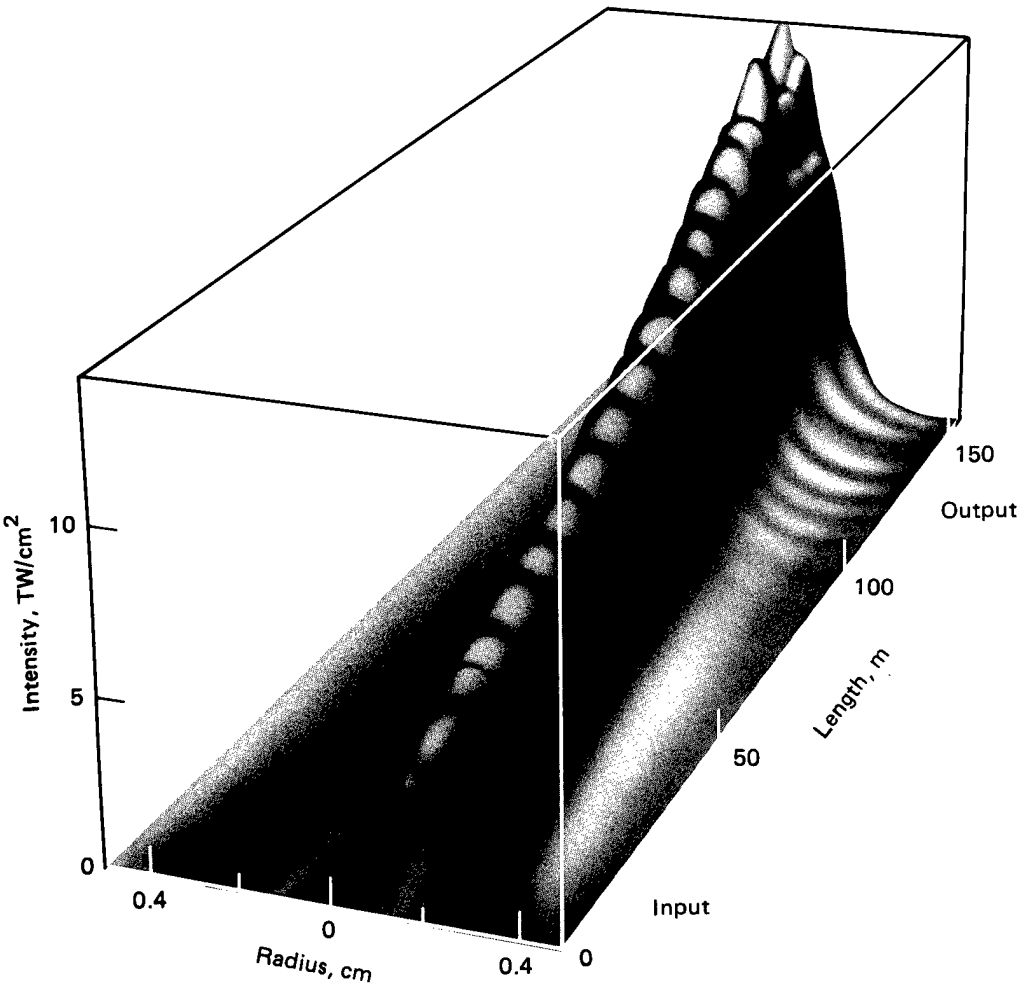

Fig. 4

Intensity of the laser field predicted by our two-dimensional FEL simulation. The long axis shows distance down the amplifier. Results indicate that the beam will propagate through a long amplifier.

losses in conventional laser systems—by enabling propagation of the laser beam directly onto a fusion target. This means that we would need an output beam width roughly equal in diameter to the target.

The performance specifications of a typical FEL driver for an ICF system are listed in Table 1, which includes the corresponding parameters of an electron accelerator. This particular device was designed for a near-ultraviolet (250-nm) laser. In a one-dimensional simulation, the output of each amplifier is 100 kJ in 15 ns. The variable-wiggler FEL amplifier is 120 m long and consists of an array of samarium-cobalt permanent magnets with a maximum field strength of 5 to 10 kG at the pole faces. Figure 5 gives a cutaway view of the device.

We have examined the requirements for an accelerator capable of delivering electrons to the FEL with the necessary energy and are studying two candidate systems. The first, technically the least

Table 1 Performance specification for a near-ultraviolet (250-nm) FEL fusion driver.

Parameter	Value
Amplifier	
Length, m	120.0
Wiggler spacing, cm	15.0
Wiggler field (variable, kG)	2.5-5.0
Beam intensity	
In, GW/cm^2	10.0
Out, TW/cm^2	42.0
Energy out, kJ (15 ns, 0.5-cm diam)	100
Accelerator	
Voltage, GeV	1.1
Current, kA	20.0
Energy spread, %	0.5
Emittance (normalized), rad-cm	0.1
Pulse length, μs	0.5-0.6

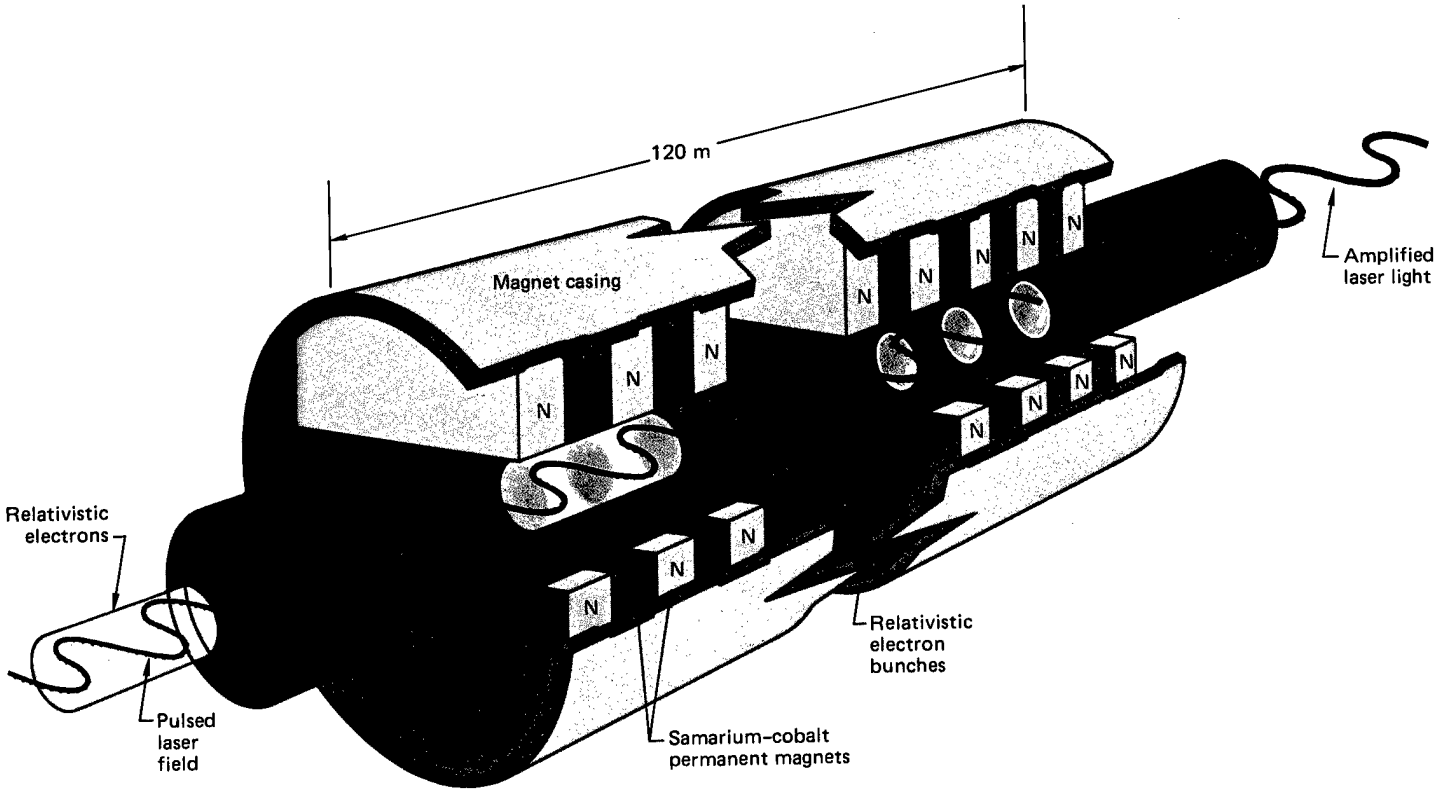

Fig. 5

Artist's conception of a typical FEL device. The wiggler consists of a series of a series of samarium-cobalt magnets 120 m long. A beam of high-energy (relativistic) electrons enters the device together with a pulsed laser field. At a certain distance along the wiggler, the kinetic energy of the electrons (now bunched as described in Fig. 3) is transferred to the laser field.

To achieve the roughly 3-MJ output required for an ICF power plant, it would be necessary to couple as many as 30 . . . 100-kJ FEL amplifiers configured to converge on a fusion target.

demanding, is a 1.1-GeV linear induction accelerator. In a linear induction accelerator, the electron beam passes through the centers of a linear array of toroids (cores) of magnetic material (ferrite). Each core is a transformer in which a pulsed power source drives the primary winding and the electron beam forms the secondary "winding." The voltage of each core is added to the electron beam as it passes down the accelerator.

At present, the most powerful accelerator of this type is the 50-MeV, 10-kA Advanced Test Accelerator (ATA) now under construction at LLNL.[5] A 1.1-GeV, 20-kA linear induction accelerator would require a significant advance over the ATA with regard to voltage and emittance. (Emittance is related to both the degree of synchronism achievable and to the fraction of electrons in a cluster that end up in the decelerating bucket.) The required voltage and current can be provided by a relatively straightforward increase in the amount of magnetic material used, pulsed power, and accelerator length. Further development would be required to satisfy the emittance requirement.

Our second candidate accelerator, attractive because of its lower cost and potentially higher efficiency, is a 1.1-GeV betatron accelerator. As in the linear induction accelerator, the electron beam forms the secondary of a transformer. In the betatron, however, electrons are accelerated in an evacuated ring. A set of bending magnets forces the beam to circulate around the betatron's magnetic core material for several thousand transits.

Use of the betatron as an electron source raises three major technical problems related to injecting electrons of sufficiently high energy into the betatron ring, extracting the high-energy beam from the ring, and maintaining beam stability in the ring during acceleration.

The injection problem can be addressed by injecting electrons into the betatron at 50 to 100 MeV from a linear induction accelerator with a pulse length equal to the transit time around the ring. The electron beam can be extracted from the betatron ring with a magnetic switch, but

the strength and volume of the required magnetic field limits the rise time of the switch to 30 ns, leading to a loss of electrons. However, the most crucial problem with the betatron remains the instability of the circulating beam at low electron emittance. This may prove intractable.

To achieve the roughly 3-MJ output required for an ICF power plant, it would be necessary to couple as many as 30 of the 100-kJ FEL amplifiers shown in Fig. 5, configured to converge on a fusion target. Figure 6 schematically represents one half of such a device (the electron

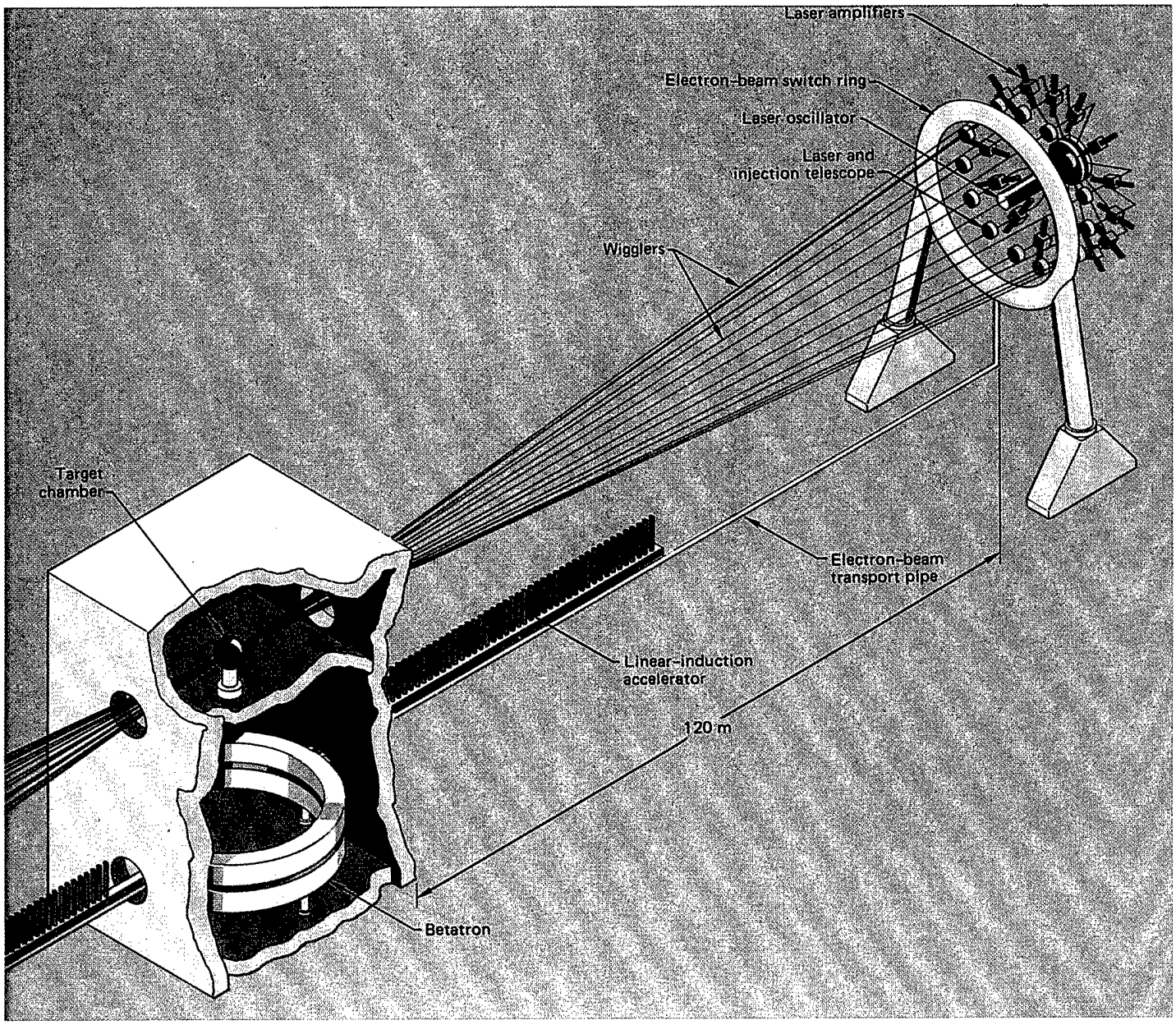

Fig. 6

Schematic drawing of a hypothetical 3-MJ ICF power plant using FEL technology. Up to 15 FEL amplifiers are configured to converge on a fusion target. The wigglers consist of laser pipes surrounded by magnets. The laser preamplifier subsystem consists of up to 15 small krypton-fluorine lasers. A grazing-incidence optical telescope in each preamplifier focuses the laser beam to provide 150 J/cm^2 as the beam is injected into the pipe aperture. All optical components are more than 130 m from the target chamber. The electron source is a 1.1-BeV betatron. Preaccelerated electrons enter the betatron from a 50-MeV linear-induction accelerator, are accelerated, and exit into a switch ring. Fast (3-ns) magnetic switches in the ring divide the relatively long accelerator pulse into as many as fifteen 15-ns flat electron-beam pulses. These shortened pulses are then magnetically guided into the wigglers.

Relativistic Effects for a Moving Electron

The Lorentz contraction is predicted by Einstein's special theory of relativity. Consider an electron moving with a velocity v_z relative to an object (in this case, the wiggler) of spacing λ_w (as measured by a stationary observer). In the electron's frame of reference, the wiggler will appear to have a length $\lambda'_w = \lambda_w/\gamma_z$, where

$$\gamma_z = \frac{1}{[1 - (v_z/c)^2]^{1/2}} ,$$

c being the speed of light. Thus, the apparent spacing of the wiggler will decrease in the electron's frame of reference.

In classical physics, the Doppler shift is the phenomenon whereby, for example, the whistle of a train moving toward a stationary observer appears to have a higher frequency than if the train were moving away. In the relativistic analogue of this effect, if radiation has a wavelength λ'_s in a moving frame of reference, it will have a wavelength

$$\lambda_s = \lambda'_s/2\gamma_z ,$$

in the frame of reference of a stationary observer (see box on p. 22).

To apply these effects to the FEL, we assume that in the electron's frame of reference the radiation wavelength is the same as the spacing of the wiggler, so that

$$\lambda'_s = \lambda'_w .$$

Applying the Doppler and Lorentz effects to translate this relationship to the laboratory's frame of reference, we obtain

$$2\gamma_z\lambda_s = \lambda_w/\gamma_z ,$$

or

$$\lambda_s = \lambda_w/2\gamma_z^2 .$$

As γ_z may easily have a value of several hundred, a 4-cm wiggler spacing could produce radiation in the visible region of the spectrum (500 nm).

source is a betatron plus a linear induction accelerator). Up to 15 evacuated laser pipes surrounded by wiggler magnets converge in a cone aimed at the target.

The laser preamplifier subsystem consists of up to 15 small krypton-fluorine lasers, one for each laser pipe. A grazing-incidence optical telescope in each preamplifier focuses the laser beam to provide 150 J/cm^2 as the beam is injected into the pipe aperture, without exceeding 10 J/cm^2 at any optical surface. The laser output of each preamplifier proceeds directly through its pipe to the target. The only optical components in the system are in the laser preamplifiers and the telescopes, both of which are more than 130 m from the target chamber.

We estimated component and total costs for a 3-MJ ICF power plant based on the two candidate systems described above (Table 2). An eventual choice among candidate technologies will depend, among other things, on success in solving the associated technical and

Table 2 Nominal subsystem costs for two candidate 3-MJ FEL fusion drivers.

Subsystem	Linear induction accelerator, $ million	Betatron, $ million
Accelerator	235	165
Magnets	15	15
Pumps	10	10
Oscillators	5	5
Building	75	75
Total	340	270
Total/MJ	110	90

Table 3 Estimated technology efficiency of two candidate systems for a near-ultraviolet (250-nm) free-electron laser fusion driver.

Technology	Linear induction accelerator, %	Betatron, %
Pulsed power to B-field[a]	60	80[b]
Transfer to e-beam[c]	85	90
Stacking[d]	85	75
Fill factor[e]	80	80
FEL extraction[f]	38	38
Overall	13	16
Overall[g]	14	18

[a]Transfer efficiency from the wall plug to the accelerating magnetic field.
[b]Probably requires some recovery of energy stored in the magnetic field.
[c]Field energy coupled into the electron beam.
[d]Energy loss incurred by dividing one long pulse into many short pulses and then recombining (stacking) the latter on the target.
[e]Optimistic estimate of spatial overlap of the electron and laser beams; this will be revised as a result of our two-dimensional propagation studies.
[f]Calculated from our one-dimensional simulation.
[g]Includes recovery of thermal energy from spent electron beam.

engineering problems and on the impact of solutions on relative costs.

Table 3 gives the estimated efficiency of several technologies used in the linear-induction accelerator and betatron designs. At this point, the betatron design appears to have an overall efficiency edge of about 20% over the linear-induction accelerator design. The efficiency of both designs might be increased slightly by thermally converting the spent electron beam to electricity at 30% efficiency. Directly recovering the energy in the spent beam would be more efficient than thermal conversion but probably would be very expensive. Some of these estimates may be revised as a result of our two-dimensional propagation studies.

Conclusions

Preliminary experiments suggest the feasibility of the FEL as a source of high-power coherent radiation. The basic technology is now undergoing intensive research and development in the laser community. Favorable resolution of the challenging technical issues would open a new range of commercial and military applications for laser-based systems. We believe that prospects are encouraging for the eventual development of FEL amplifiers with the short wavelengths and high peak power required for a commercial-scale ICF power plant. Our studies suggest that such plants could combine high conversion efficiency with relatively low cost.

Key Words: electron-beam accelerator; energy conversion; free-electron laser; intertial confinement fusion.

Notes and References

1. First proposed by H. Motz, "Applications of the Radiation from Fast Electron Beams," *J. Appl. Phys.*, **22**, 527 (1951), and demonstrated by D. A. G. Deacon, L. R. Elias, J. M. J. Madey, G. J. Ramian, H. A. Schwettman, and T. I. Smith, "First Operation of a Free-Electron Laser," *Phys. Rev. Lett.*, **38**, 892 (1977).
2. For a review of the Laboratory's Nova laser fusion program, see the December 1980 *Energy and Technology Review* (UCRL-52000-80-12), p. 1.
3. D. Prosnitz, A. Szoke, and U. K. Neil, "High-Gain, Free-Electron Laser Amplifiers: Design Considerations and Simulation," *Phys. Rev. A*, **24**, 1436 (1981).
4. N. M. Kroll, P. L. Morton, and M. N. Rosenbluth, "Free-Electron Lasers with Variable Parameter Wigglers," *IEEE J. Quantum Electron.*, *QE-17*, 1436 (1981).
5. The Advanced Test Accelerator was described in *Energy and Technology Review*, UCRL-52000-81-12 (December 1981), p. 1.

Magnetic Compressors: High-Power Pulse Sources

We are anticipating future needs beyond the capabilities of the spark-gap switches we developed for the Advanced Test Accelerator (ATA). We are continuing our efforts on magnetic pulse compressors that use nonlinear magnetic components and have designed reliable, high-current pulse compressors capable of generating continuous, 50-ns, 250-kV pulses at repetition rates exceeding 1 kHz. The use of new circuit designs and metallic glasses in these compressors will help us produce pulses with even higher repetition rates.

The Laboratory's Advanced Test Accelerator (ATA),[1] funded by the Defense Advanced Research Projects Agency, is a 50-MeV, 10-kA induction linear accelerator. The pulse of its output electron beam lasts up to 50 ns and can be repeated once a millisecond for up to ten pulses. This ten-pulse burst can be repeated every two seconds, giving the machine an average repetition rate of five pulses per second.

This performance, which makes the ATA unique among pulse power machines, came as the result of research on a novel, coaxial, gas-blown spark gap. The ATA contains modular, 250-kV induction-accelerator cells, each driven by a single pulse power unit. Each unit consists of a resonant transformer (1:10 step-up), a water-filled Blumlein pulse-forming line (PFL) for energy storage, and the aforementioned spark gap to discharge the PFL into the accelerator cell.

The initial commutation in the chain is performed by six fast-recovery, glass-envelope thyratrons, four operating in the forward and two in the reverse direction. These tubular thyratrons, specially made for high-peak-power, low-duty-factor applications, transfer energy held in intermediate storage through the 1:10 transformer and into the PFL. The transfer is completed in 20 μs, and the tubes recover their ability to hold voltage in another 20 μs.

A hiatus of 1 ms or more between pulses is necessary so the discharge products can be blown out of the spark gap. In theory, higher repetition rates could have been achieved by increasing the velocity of the gas that blows them out. Any significant increase is impractical, however, since the power required from the blower scales as the

For further information contact Daniel L. Birx (415) 422-7091.

Fig. 1

A comparison of the pulse power requirements of various accelerators. Radio-frequency voltage and power at various locations in the pulse-forming network (a) in the Stanford Linear Accelerator, (b) in the ATA induction linear accelerator, and (c) in a comparable nonlinear magnetic drive.

cube of the repetition rate, and it is already at 11.2 kW per gap for 1-kHz operation.

Figure 1, which schematically compares the pulse power requirements for the ATA and the Stanford Linear Accelerator (SLAC), suggests part of the reason why we needed to use spark gaps in the ATA. Although the pulse energy supplied to a SLAC radio-frequency accelerator section is essentially the same as that supplied to an ATA induction cell, the power level to the ATA is about a hundred times larger because the pulse is so much shorter.

The energy compression supplied by the spark gap (switch S_2 in Fig. 1b) supplies this power gain. A spark-gap switch consists of a coaxial anode and cathode with a trigger electrode between. The switch, which is filled with gas at high pressure, closes on command when the trigger electrode is pulsed, causing a breakdown arc within the gas, which then conducts current. The combination of a 250-kV operating voltage and a requirement for a current rise of 1 TA/μs (or 10^{18} A/s) forced us

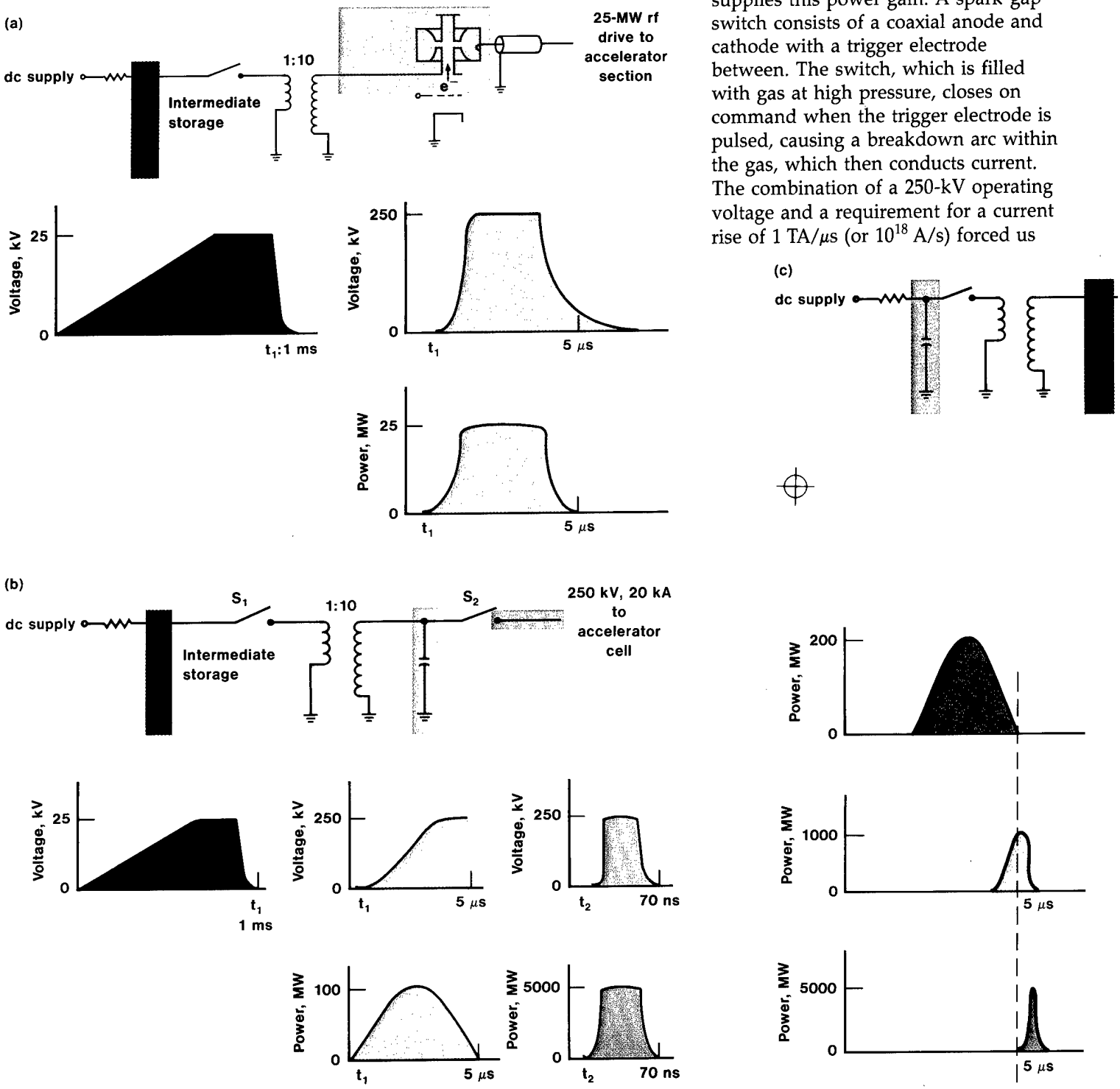

to use the crude but effective high-pressure spark-gap technology. However, such technology is not adequate to achieve high repetition rates for future applications. It appears to be a rule of nature that the designed repetition rate will never be high enough; experimenters will always find reasons for wanting to go higher.

Research into alternative switching schemes began almost before the first spark gaps went into use. At first, we tried to develop a high-power version of the thyratron (switch S_1 in Fig. 1b). A thyratron is a triode (similar in design to a vacuum tube) filled with deuterium at low pressure. It operates as a closing switch, ionizing the deuterium, when the grid (one of the three electrodes) is pulsed. Such a low-pressure gas switch certainly seemed to embody the technology most likely to meet our requirements.

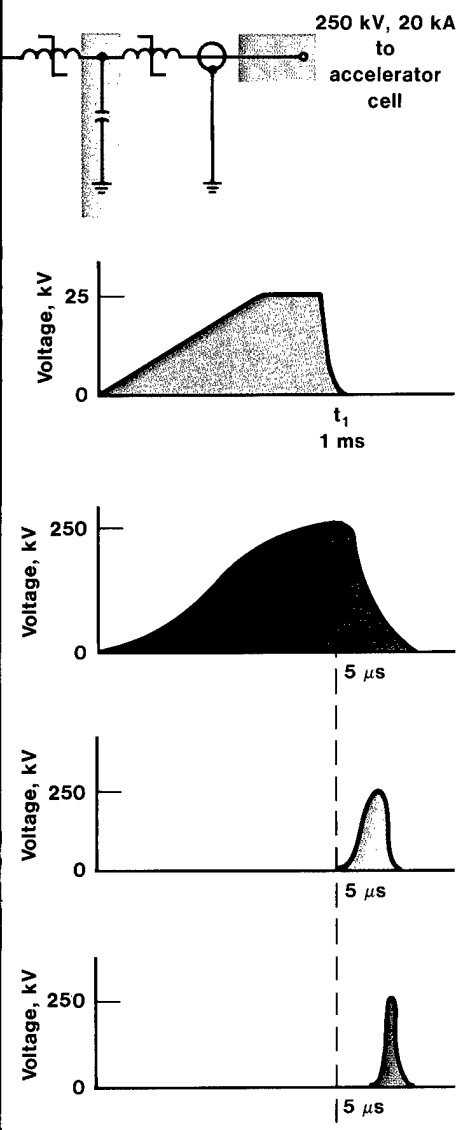

This work provided us with invaluable insights into the physics of low-pressure gas switches. It also demonstrated that such a switch, while possible in concept, is impractical. Because of its size and expense, it would have been only a slight improvement over several hundred conventional thyratrons operating in a series-parallel configuration.

This realization would have come as a disappointment if we had not, on the way to developing the super thyratron, discovered something much better. We had been experimenting with saturable inductors to ease the rise-time requirements on our low-pressure switches (an idea gleaned from reports dating back to the 1950s), and they turned out to be far more effective than we had expected. We found that we could reduce the voltage and rise-time requirements enough to eliminate the need for a high-power switch. This idea, schematically depicted in Fig. 1c, made it possible to stay with conventional thyratrons.

Magnetic Pulse Compression

The basic circuit for magnetic pulse compression is essentially the same as originally conceived in the 1950s. The fundamental principle involved is to use the large changes in permeability exhibited by saturating ferri-(ferro-)magnetic materials to produce large changes in impedance. Figure 2a shows the permeability changes in a representative saturable magnetic material, and Fig. 2b illustrates the standard technique for capitalizing on this behavior. First, a repetitive power source (using existing technology) generates the initial pulse. As this pulse propagates through the network, it goes through several states of compression until it achieves the desired output shape.

By using multiple stages as shown, it is possible to achieve a much larger effective change in impedance than can be obtained from a single stage. In fact,

the effective change in impedance is limited only by the physical layout and materials properties. Figure 2c illustrates the results of the compression process.

The operation of this circuit can be described as follows. Capacitor C_1 charges through inductance L_0 until inductance L_1 saturates, becoming much less than L_0. Once this happens, C_2 will begin to charge from C_1 through $L_{1\,sat}$, but since $L_{1\,sat}$ is much less than L_0, C_2 charges more rapidly than C_1 did. This process continues through the successive stages until C_n discharges into the load through $L_{n\,sat}$.

Fig. 2

Diagrams outlining the operation of magnetic pulse compression. (a) The hysteresis *(B–H)* loop of a typical saturable magnetic material. (b) Simplified schematic of a magnetic pulse compressor. The elements marked L_1, L_2, and L_n are nonlinear inductors. (c) Typical voltage waveforms associated with a magnetic pulse compressor.

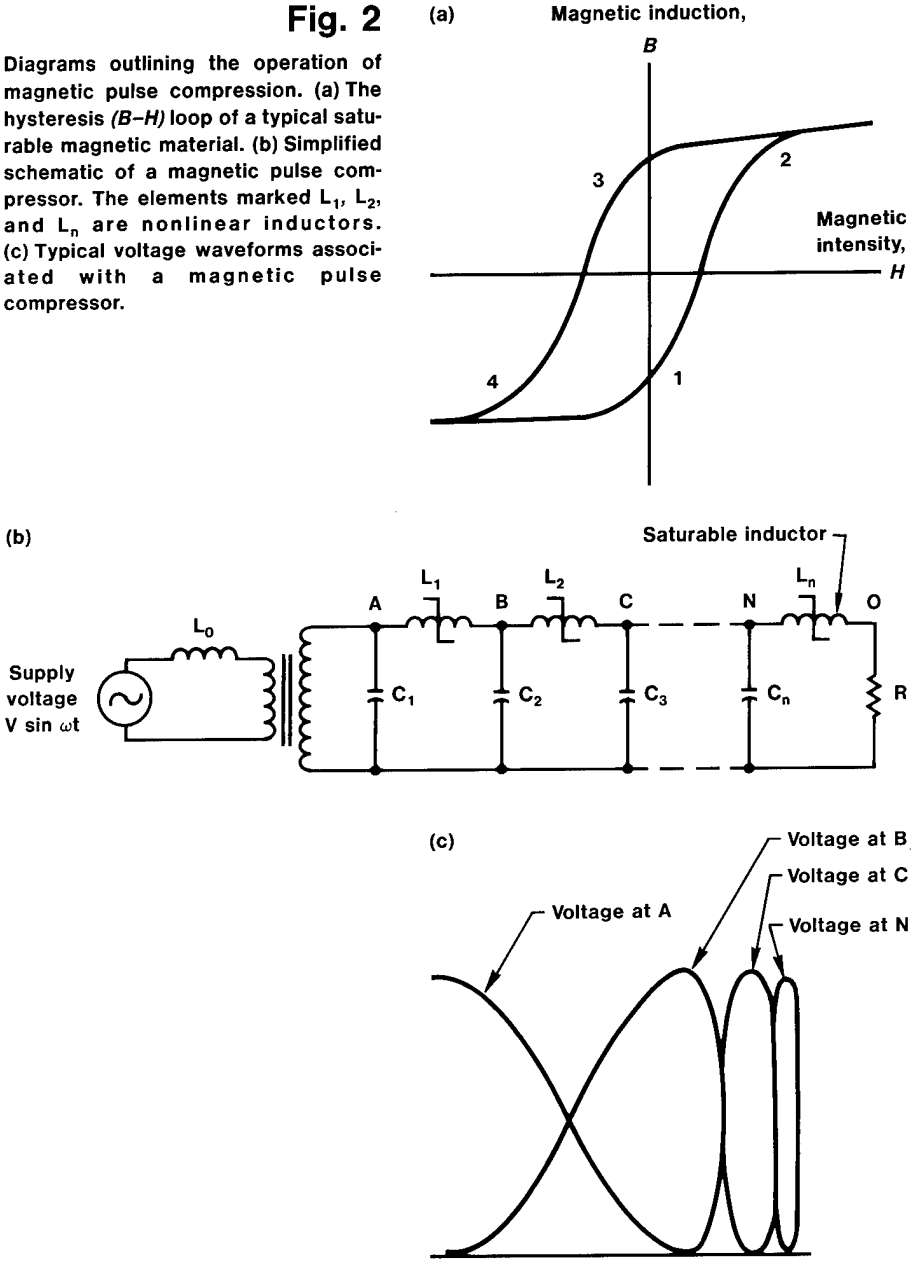

To make this process efficient, we design each of these successive stages so that saturation occurs at the peak of the voltage waveform. Segment 1 to 2 in the hysteresis loop of Fig. 2a is the active or high-permeability region during which the inductor impedes current flow; the leveling off of the curve at point 2, reached at the peak of the voltage waveform, indicates core saturation when the inductor achieves a low impedance. During segment 2 to 4, the core is reset to its original state, ready for the next cycle.

The research and development effort that followed this discovery produced several primitive pulse power units based on magnetic compression. Even these early efforts proved to be such an improvement over the spark-gap switches that a few of them were installed in critical areas of the ETA and ATA, and all are still in operation.

Because pulse compressors are passive devices, their operation requires an initial pulse, which we usually obtain by discharging an intermediate storage capacitor through one or more thyratrons. Figure 3 outlines various methods of achieving high repetition rates with this general arrangement. Most of our pulsers operate in the simple command resonant charge mode, and the time required to recharge the intermediate storage capacitor combined with thyratron recovery times limits operation to about 15 kHz.

Aside from creating the ability to operate at increased repetition rates, the installation of magnetic pulse compressors appeared warranted on the basis of reliability and low maintenance. The benefits to the experimental program were also considerable.

The ATA Upgrade Prototype

Since October 1980, when we first began to work with magnetic switches, we have completed installation and final testing of a prototype magnetic switch package to replace the spark gaps in the ATA power units. The challenge was not to prove that a

magnetic switch would do the job but rather to produce a unit that would fit the existing space, use as much of the existing equipment as possible, and be as inexpensive and reliable as possible.

The problem was further complicated by a desire for a peak repetition rate exceeding several kilohertz and an average repetition rate of at least 100 Hz. We also wanted the ability to operate at 1 kHz for up to one minute in every ten to enable us to use the ATA for high-power, free-electron-laser experiments.

Figure 4 compares the two systems for driving ATA cells, the original one (containing a resonant transformer, a gas-blown spark gap, and a Blumlein line) and the new pulse compressor based on nonlinear magnetic elements. The latter is relatively inexpensive, and its performance surpasses that of any other system. Table 1 partially documents the capabilities demonstrated by this prototype.

Figure 5 compares the physical dimensions of the two systems. The existing pulse power unit is somewhat shorter than the new magnetic replacement, but it drives only one cell instead of two. The new unit consists of an input step-up transformer, one stage of compression to charge the transmission line, a second stage of compression, and the output coupling transformer. The output transformer can be housed as part of the magnetic pulse generator or as part of the load for best impedance matching.

Adding coupling transformers at both the input and the output of the magnetic pulse compressor improves the system's versatility by permitting it to achieve the desired output pulse while allowing the compression stages and the input switching device to operate at their most efficient values of voltage and current.

At this point in the evolution of the pulse-shaping hardware, we can design the transformer turns and the interstage capacitors as integral parts of the system. The resulting magnetic compressor is simple and extremely reliable, and it satisfies all the required performance specifications.

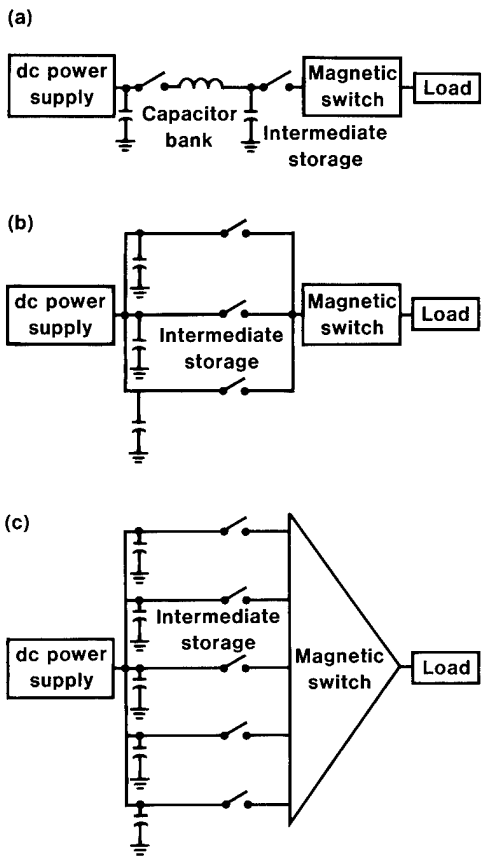

Fig. 3

Three kinds of magnetic compressor for use at high repetition rates. (a) The command resonant charge system, used up to 10 kHz. Both switches must recover before the unit can be pulsed again. (b) The Gatling-gun mode, used up to 30 kHz. Only one switch must recover before the unit is pulsed again, which increases the repetition rate. (c) Branched magnetics for producing a pulse with a high repetition rate (50 MHz). No switch recovery is required before the unit is pulsed again.

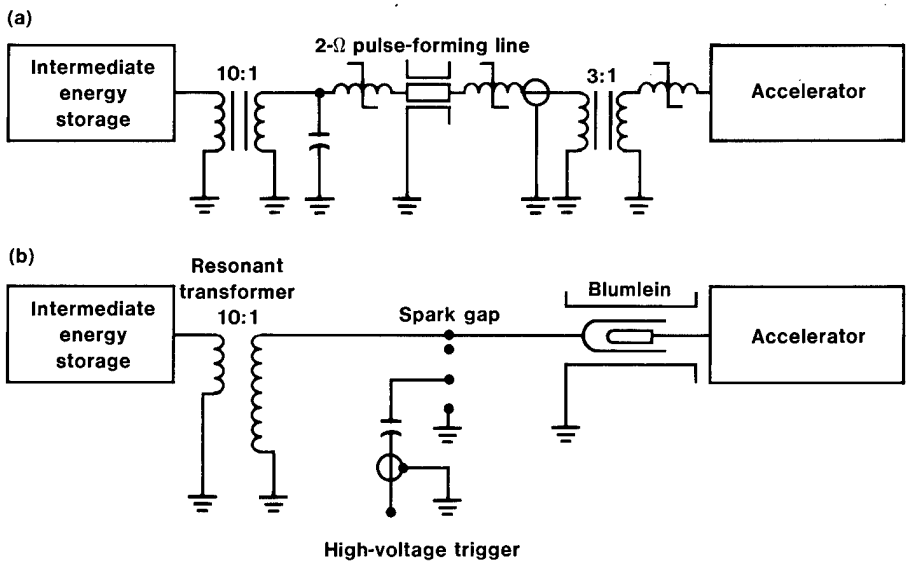

Fig. 4

Simplified schematics of pulse power chains for the ATA induction linear accelerator. (a) The present system, which uses a spark gap and Blumlein pulse formers. (b) The nonlinear magnetic drive proposed for an upgrade of the ATA.

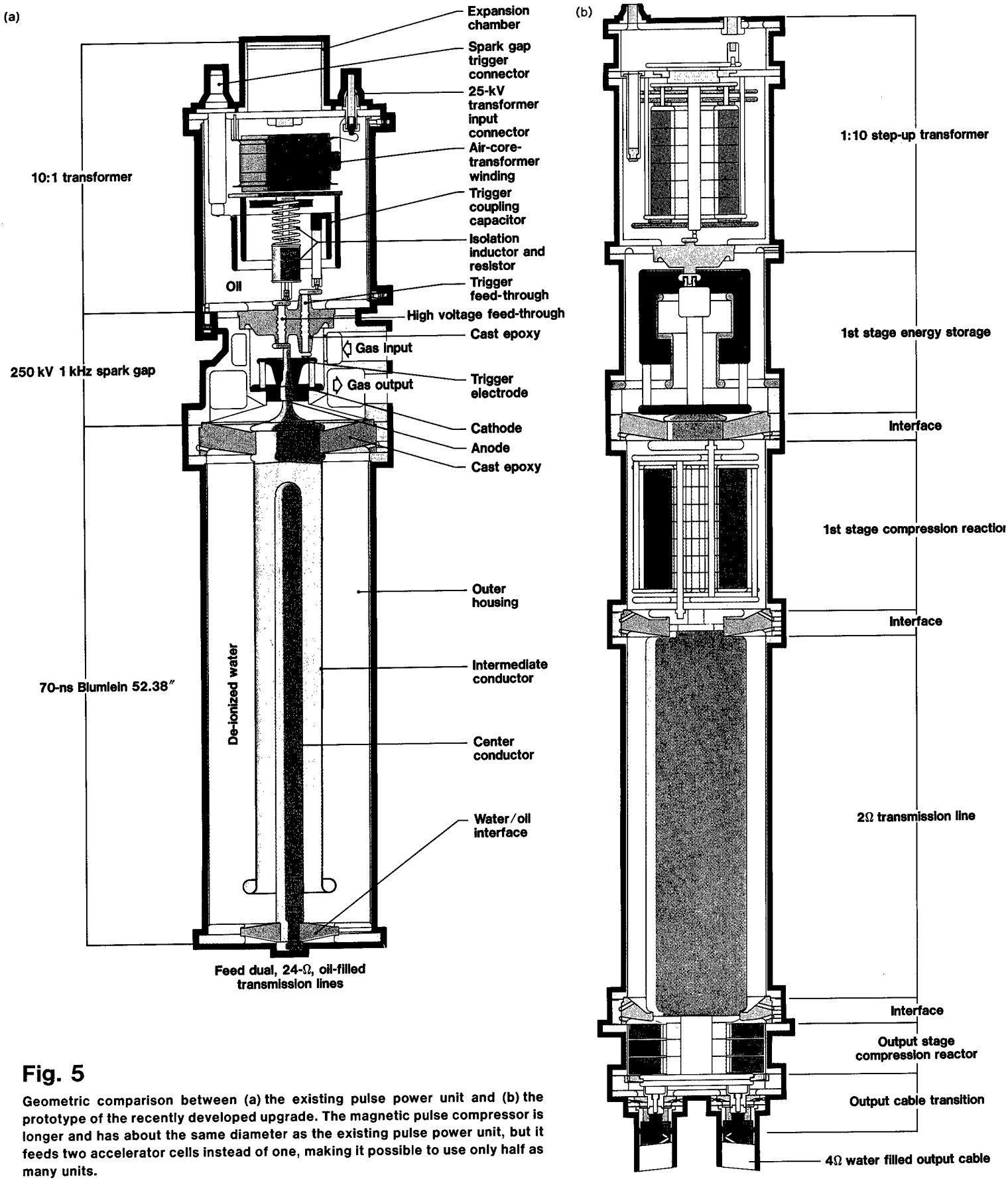

Fig. 5

Geometric comparison between (a) the existing pulse power unit and (b) the prototype of the recently developed upgrade. The magnetic pulse compressor is longer and has about the same diameter as the existing pulse power unit, but it feeds two accelerator cells instead of one, making it possible to use only half as many units.

Table 1 Comparison of output pulse parameters of the current spark-gap driver of the Advanced Test Accelerator and the MAG-1 prototype of an upgraded magnetic compression system.

Parameter	Spark gap	Magnetic compression
Peak output power, GW	2.5	10
Pulse rise time (10%-90%) per cell, ns	18	15
Pulse length (FWHM), ns	70	80
Pulse energy, J	350	800
Efficiency (including resonant transformer), %	70	80
Voltage (2-cell driver) at 18 kA/cell, kV	100	300
Voltage (1-cell driver) at 25 kA/cell, kV	200	450
Pulse-to-pulse jitter at up to 1 kHz, ns	±1	±0.5
Peak burst rate (5 pulses), kHz	1	>10
Peak average repetition rate at 10% duty factor, kHz	0.1	1

A desire to double the individual accelerator-cell voltage, coupled with the difficulty of sending 500-kV pulses around the system, prompted us to adopt an alternate procedure. We send the output from the magnetic driver (about 170-kV peak) down to the accelerator cells via two 4-Ω, semirigid, water-filled transmission lines. There, a pulse transformer provides a 3:1 voltage step-up and a ferrite pulse sharpener steepens the rise time. Figure 6 shows the physical layout and the two voltage waveforms. Saturation of the ferrite in the cell core further shortens the waveform of the cell voltage. These cells are now operated at 250 kV for 50 ns and will probably need to be modified by having the ferrite core replaced with one wound from metallic glass, if operation at the full capability of the magnetic compressor (500 kV per cell) is desired.

Metallic Glasses

The most critical aspect of the magnetic pulse compressor, in terms of achieving both high efficiency and fast rise times, is the material in its final stages. The only material that satisfies all of the requirements for these final stages is one or another of the new ferromagnetic metallic glasses.

In systems with low repetition rates, the overall power efficiency of the magnetic pulse compression stages is

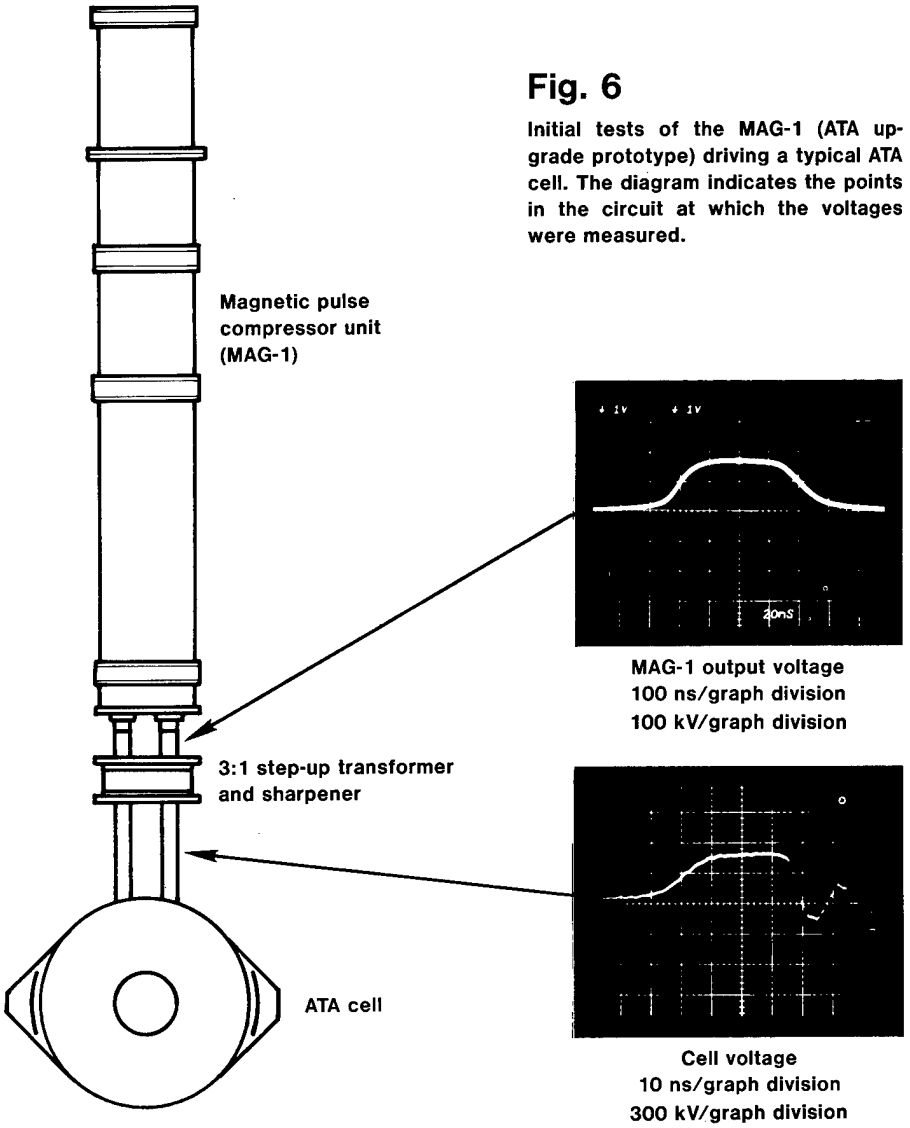

Fig. 6

Initial tests of the MAG-1 (ATA upgrade prototype) driving a typical ATA cell. The diagram indicates the points in the circuit at which the voltages were measured.

Fig. 7

Simplified circuit diagram of the burst-mode pulse generator designed to provide any desired repetition rate for a fixed number of pulses (in this case, eight). The numbers indicate the order in which the capacitors are discharged. In this pulse generator, an example of the type illustrated in Fig. 3c, no switch recovery is required after pulsing before the unit is pulsed again.

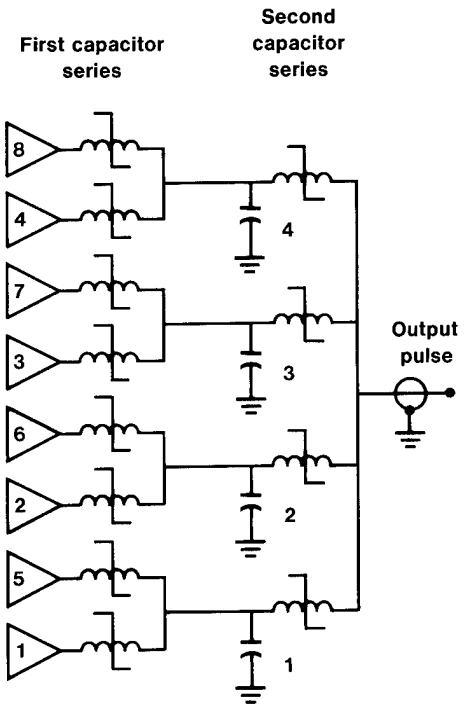

not critical. Even our original, unoptimized pulse compressors, which were built from nickel-iron and ferrite left over from previous projects, achieved efficiencies of more than 50%. Our most recently constructed magnetic compressors, which have metallic glass cores, achieve efficiencies greater than 80%. In systems with high repetition rates, high efficiencies are necessary to reduce internal losses and heating, which affect the life of the components.

The rebirth of the pulse compression technique as a highly reliable source of pulses of very high power and high repetition rate is due in large part to this new amorphous material. Metallic glass offers all the necessary properties of high saturation, high resistivity, and rapid transition from high to low permeability that make the magnetic compressor so attractive. Commercial availability of this material at about the time we needed it also made magnetic compression very practical.

Metallic glass is a generic term for metals that have been solidified so rapidly (about a million degrees per second) that they have no time to form the usual crystal structure. The process is done commercially by directing a thin jet of the molten metal or alloy onto a chilled, rapidly rotating metal disk or cylinder. This automatically forms a ribbon of metallic glass about 25 μm thick, which spins off at a very high rate. Most of the material we use in our magnetic compressors is iron-based or an alloy of cobalt and iron that yields a higher saturation flux.

For short pulses, the dominant factor contributing to core losses is the presence of eddy currents. These losses scale as the square of the core material's thickness and inversely as its resistivity. Amorphous metals have resistivities about three times higher than the same material in crystalline form and can be mass produced in ribbon less than 28 μm thick, making them ideal for generating fast pulses with high efficiency.

Going to Higher Repetition Rates

The type of magnetic pulse generator discussed so far consisted of a repetitive pulse source and several serial stages of pulse compression. Such a system can supply a burst with any number of pulses or can operate continuously. The burst rate, as already mentioned, is established by thyratron recovery times. If the requirement is for a fixed number of pulses in a burst, however, then a new scheme of pulse generation becomes feasible.

This scheme involves a number of parallel storage capacitors and switches that are fired in sequence at practically any repetition rate. The circuit for such a magnetic burst generator, in which portions of the eight forward pulses are used to reset the saturable inductors in

Fig. 8

Output waveforms from a low-power test of the burst-mode pulse generator, operating at a repetition rate of 16 MHz (eight pulses in 500 ns).

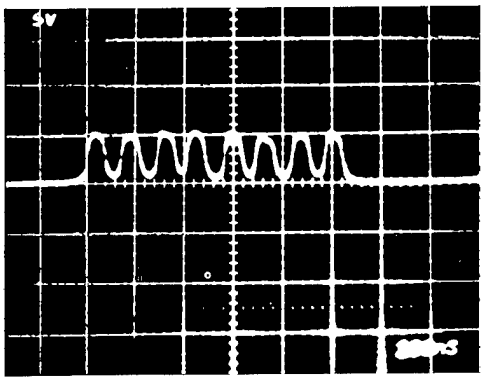

100 ns/graph division

the circuit between pulses, is shown in Fig. 7. This eight-pulse burst generator is essentially a two-stage magnetic compressor with eight first stages and four second stages all feeding into one output load.

The timing between the output pulses is simply determined by the time delay between triggering the successive SCRs (silicon controlled rectifiers, solid-state devices analogous to thyratrons). The output capacitors consist of varying lengths of RG58 coaxial cable. The timing delays between the triggering of the SCRs was determined by cable lengths. Figure 8 shows the summed output pulse from a 60-ns length of cable, which crams an eight-pulse burst into a 500-ns interval for an effective repetition rate of 16 MHz.

Although this initial proof-of-principle experiment was performed at low power, there is no apparent barrier to scaling it up indefinitely. Therefore, this technique of burst generation offers a way to build high-power pulse generators with essentially unlimited repetition rate.

Conclusion

An old technology (pulse compression) applied to a new magnetic material (metallic glass) is enabling us to develop a pulsed power system that is reliable and efficient and that can be adapted to drive accelerators with a wide range of performance specifications. By adding a high-peak-power switch to initiate the compression chain, we reduced the total number of stages and produced a simpler, more efficient magnetic pulse generator. This higher efficiency makes it possible to operate an induction accelerator continuously with extremely high average power. The former repetition rate limitation was imposed by thyratron recovery time and not by magnetic properties. We have also developed a new magnetic pulse generator, operating in bursts, that magnetically isolates the recovery time of the switching device, allowing practically unlimited repetition rates. In short, magnetic pulse compressors are ideally suited for driving low-impedance induction accelerators with short pulses (70 ns), short rise time (15 ns), and high peak power (10 GW) at any desired repetition rate.

Key Words: amorphous magnetic material; Advanced Test Accelerator; (ATA); Experimental Test Accelerator; (ETA); magnetic pulse compression; metallic glass.

Notes and References

1. For more information on the Advanced Test Accelerator, see the December 1981 *Energy and Technology Review* (UCRL-52000-82-12), p. 1.

Prepared for DOE under contract No. W-7405-Eng-48

Work performed under the auspices of the U.S. Department of Energy by Lawrence Livermore National Laboratory under Contract W-7405-Eng-48.

☆ U.S. GOVERNMENT PRINTING OFFICE: 1984—790-056